

## Responses to reviewers' comments

We would like to thank the four reviewers for their comprehensive assessments and constructive comments on our manuscript. We include a point-by-point [response to each comment from the submitted manuscript](#) and [“proposed revisions in our revised manuscript”](#) to address the comments below. The annotated line numbers refer to the preprint version of the manuscript.

We have carefully revised the manuscript to (1) expand the evaluation of the simulation using the updated offline dust emissions against measurements of surface fine dust concentrations over the US and several independent measurements of surface dust concentration over the globe, (2) supplement more technical details of the proposed method, and (3) improve logic and clarity.

We believe our response has addressed the reviewers' comments as described in more detail below.

---

### Anonymous Referee #1:

General comments:

In this paper, Meng et al. proposed a grid-independent dust emissions module for CTMs (GEOS-Chem in this case), where dust flux is being calculated a priori and offline within the emissions module (HEMCO in this case). In essence, this approach seems to be replacing the error due to interpolating meteorological fields with those due to interpolating the final dust flux. Considering nonlinear relations between meteorological fields and calculated dust fluxes, I am concerned about using this interpolated dust flux together with the interpolated meteorological fields later in a CTM to represent dust transport, diffusion, deposition, etc. The benefit of an online approach (other than the aerosol feedback) is a physical consistency between wind, relative humidity, temperature, soil moisture, etc. representing both dust emissions and other phenomena such as dust transport and deposition, and I am not convinced that the offline approach provides the same faithfulness. Along that line, I found a number of major issues both with the proposed approach as well as its evaluation as summarized in the next section.

[Response:](#) Thank you for your comment. The purpose of our manuscript may have been misunderstood. Our goal is to provide the most accurate dust emissions possible, regardless of model resolution. We have tried to more clearly motivate the manuscript. We have added text to clarify the extent of the large errors associated with existing approaches that rely on coarse resolution meteorological fields. Specifically, we have added to line 53 a clearer motivation for the offline approach [“The nonlinear dependence of dust emissions on meteorology introduces an artificial dependence of simulations upon model resolution \(Ridley et al., 2013\)”](#), and to line 55, [“Smoothing meteorological fields to coarse resolution can lead to wind speeds falling below the emission threshold in regions that do emit dust.”](#) and to line 62, [“Resolution-dependent mineral dust emission would vary by a factor of 3 from C360 to C24 \(Ridley et al., 2013\). Such large resolution-dependent biases would undermine applications of CTMs to assess dust effects, and would lead to large within-simulation inconsistency for stretched grid simulations that can span the entire resolution range simultaneously”](#), and to line 195, [“The difference between the online and offline dust emissions, shown in Fig. 2f, can be considered the error in the online approach arising from coarse resolution meteorological fields.”](#)

Specific comments:

1(a)/ If the only major benefit of the offline approach is a better resolution, simulations should be conducted with various grid resolutions rather than just contrasting the two extremes (2deg x 2.5deg vs. 0.25deg x 0.3125deg).

Response: We now emphasize that the major benefit of the offline approach is consistency across resolutions in line 283: *“The native resolution offline dust emissions facilitate consistent evaluation and application across all model resolutions”*. We also note that simulations conducted in this study are all in 2x2.5 deg, which is the most commonly used GEOS-Chem simulation resolution, as stated in line 150: *“We conduct global simulations with GEOS-Chem (version 12.5.0) at a horizontal resolution of 2° by 2.5° for the year 2016”* in Sect. 2.4.

1(b)/ Specifically, comparisons should be conducted to ensure that the online and offline techniques indeed give the exact same dust flux with the same grid resolution.

Response: Indeed, the online and offline emissions at the same base resolution (0.25° by 0.3125°) are identical by design since the offline emissions are archived from the online code.

2/ The soil moisture (another important meteorological factor) was not mentioned when using the offline approach. Wind and soil moisture are dynamically linked and should be represented and discussed.

Response: We added to line 104 for clarification that soil moisture is indeed used for offline emissions: *“The saltation process is dependent on the critical threshold wind speed, which is determined by surface roughness, soil type and soil moisture.”*

3 (a)/ Based on the scatterplots in figures 3 and 4, the offline model seems to almost always give higher dust emissions, but figure 2(f) shows considerably lower values from the offline model over the Sahara and Sahel. Please discuss this inconsistency.

Response: The purpose of Fig. 2f was to show the spatial difference between the online and offline dust emissions with the same global dust strength and the same dust source function. Figure 3 and 4 were comparing simulations with original online dust emissions and updated offline dust emissions. The original online dust emissions had a global total dust strength of 909 Tg yr<sup>-1</sup>; while the updated offline dust emissions were scaled to 2,000 Tg yr<sup>-1</sup>. We consider the simulation with the original online dust emissions as the baseline simulation. The purpose of those two comparison figures is to justify the advantage of using offline dust emissions with optimized global annual dust strength in the future simulations. We have modified the caption of Figure 3 and Figure 4 as below to make it clearer.

*“The results for the simulation using the original dust emissions are shown in blue; the results for the simulation using updated dust emissions with dust strength of 2,000 Tg yr<sup>-1</sup> are shown in red. The best fit lines are dashed.”*

3 (b)/ Also, along that line, figure 3 should include a comparison between spatial distributions of online vs offline (overlaid with the AERONET obs) AOD. Perhaps replace the DOD/AOD column and move it to the Supplement?

Response: We will add a comparison of simulated AOD overlaid with AERONET AOD between simulations with online dust emissions (Fig 2b) and offline dust emissions (Fig 2d) in the supplement as Figure S7 (Figure R1 in this response) to show the spatial difference of simulated AOD. The difference in simulated AOD reflects the differences in the emissions (Fig 2f).

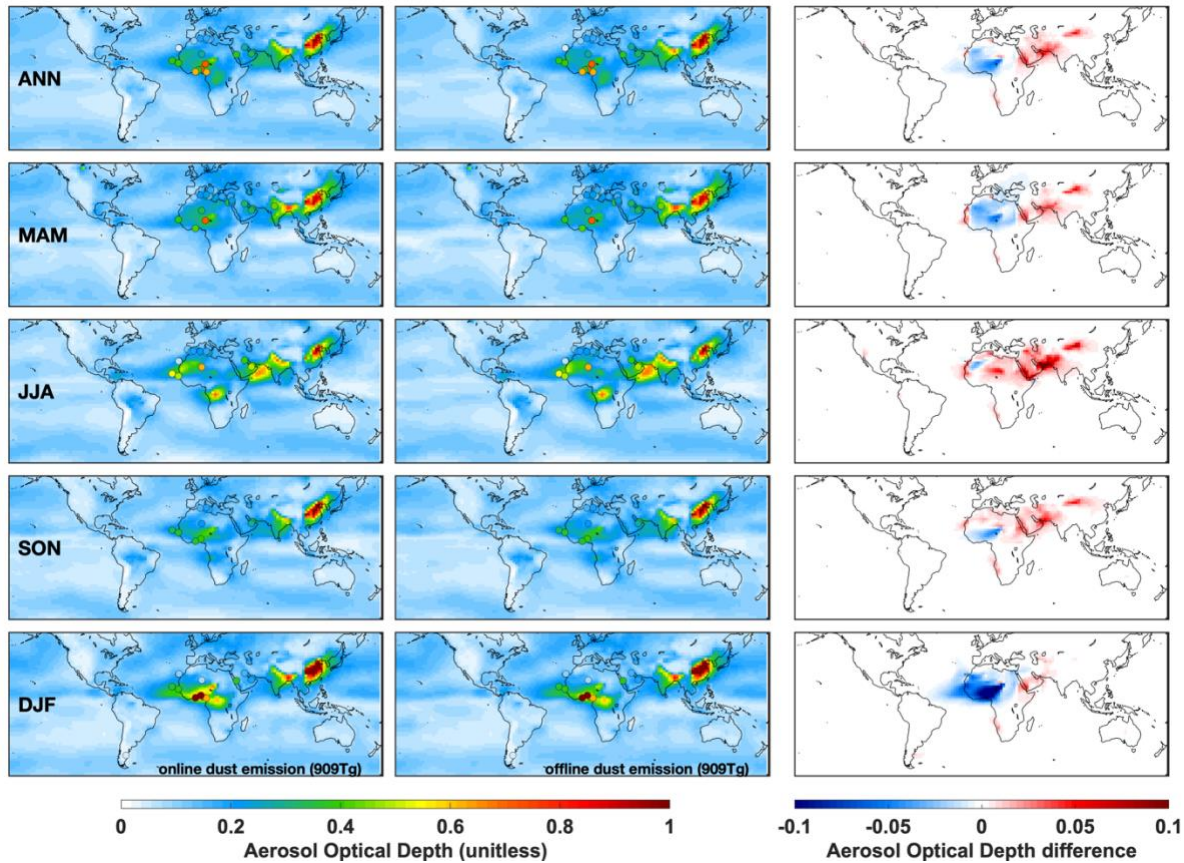


Figure R1. Spatial distribution of simulated AOD from simulations using the online dust emissions (left column) and offline dust emissions (middle column) that were with the same updated dust source function and the same annual dust strength (909 Tg), and the AOD differences between those two simulations (right column) in different seasons. Filled circles represent the AERONET measurements included in Figure 3.

We also add description in line 213 as the following:

*“Difference maps of simulated AOD between online and offline dust emissions are shown in Figure S7.”*

4/ Throughout the abstract, main text, and conclusion sections, the offline model is argued to better resolve weak dust source regions, but no evaluations are provided for these regions.

Response: We rephrased our abstract in lines 25-27 as below:

*“These updated offline dust emissions based on high resolution meteorological fields strengthen the dust emissions over relatively weak dust source regions”*

We also add evaluation with observations near weak dust source regions. We include a climatology of dust surface concentrations measurements over 1981-2000 from several independent dust measurement sites over the globe (Kok et al. 2020). We use those sites (12 in total) (Figure R2) that either in the dust belt across Northern Hemisphere or sites relatively close to the weak emission regions in the Southern Hemisphere to evaluate our dust simulation (Figure R3).

We will add Figure R3 into our main text as Figure 6. We add a new paragraph in the main text to describe the results in Figure 6:

*“Figure 6 shows the comparison of seasonal averaged modeled and measured surface dust concentrations from 12 independent sites across the globe. The simulation using the updated offline dust emissions with dust strength of 2,000 Tg yr<sup>-1</sup> is more consistent with the observations at almost all sites. The remaining bias at sites distant from source regions, for example sites in the Southern Hemisphere and East Asia, likely reflects remaining uncertainty in representing dust deposition. Further research is needed to address remaining knowledge gaps, such as better representing the dust size distribution and deposition during transport.”*

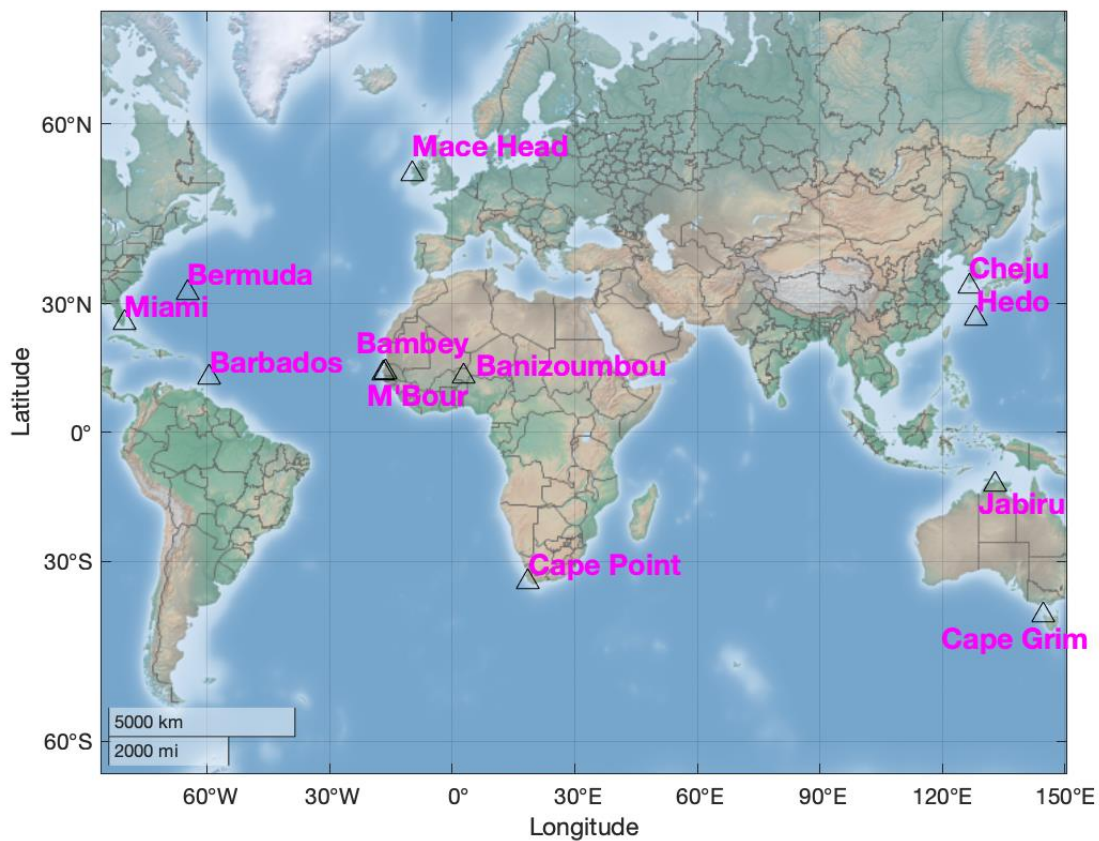


Figure R2. Geolocation of the 12 independent dust surface concentration sites.

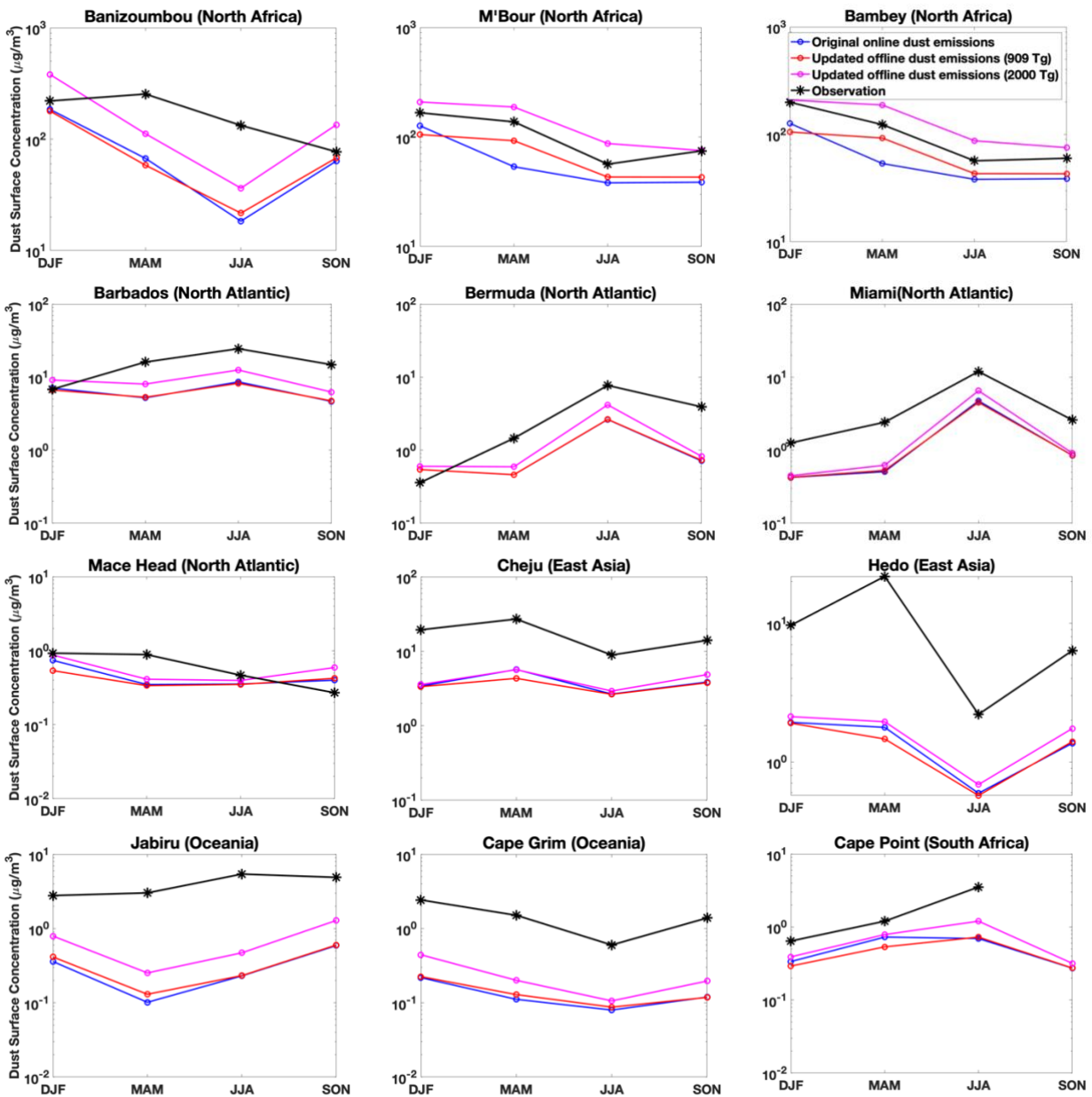


Figure R3. Comparison of modeled and measured seasonal averaged surface dust concentrations at 12 independent globally distributed sites for the years 1981-2000. Nine sites are in the dust belt across Northern hemisphere. The remaining 3 sites are relatively close to the weak dust emission regions in Southern Hemisphere. The results for the simulation using the original dust emissions are shown in blue; the results for the simulation using updated dust emissions with dust strength of 909 Tg yr<sup>-1</sup> are shown in red; the results for the simulation using updated dust emissions with dust strength of 2,000 Tg yr<sup>-1</sup> are shown in magenta. The measurements are in black.

5/ I see no connection (and in fact no scientific merit from the physics point of view) between the scaling factor and the offline approach. The scaling is not an advantage of the offline model as described in sec. 3.3. An online model can also be scaled using the parameter “C” in Eq. (1) of the Supplement. Additionally, the paper misses the justification behind the chosen scaling factors as well as a detailed evaluation.

Response:

We modified text starting from line 58 to clarify the connection between scaling factor and the offline approach: *“Addressing this nonlinearity is especially important for the next generation of chemistry transport models that is emerging with nimble capability for a variety of resolutions at the global scale. For example, the high performance version of GEOS-Chem (GCHP) (Eastham et al., 2018) currently offers simulation resolutions that vary by over a factor of over 100 from C24 (~ 4 °x4 °) to C360 (~0.25 °x0.25 °), with progress toward even finer resolution and toward a variable stretched grid capability (Bindle et al., 2020). Resolution-dependent mineral dust emission would vary by a factor of 3 from C360 to C24 (Ridley et al., 2013). Such large resolution-dependent biases would undermine applications of CTMs to assess dust effects, and would lead to large within-simulation inconsistency for stretched grid simulations that can span the entire resolution range simultaneously. Grid-independent high resolution dust emissions offer a potential solution to this issue.”*

We also add more evaluations in our main text against other types of observations, including measurements of surface fine dust concentration over the US (Figure R4) and several independent measurements of surface dust concentration over the globe (Figure R3).

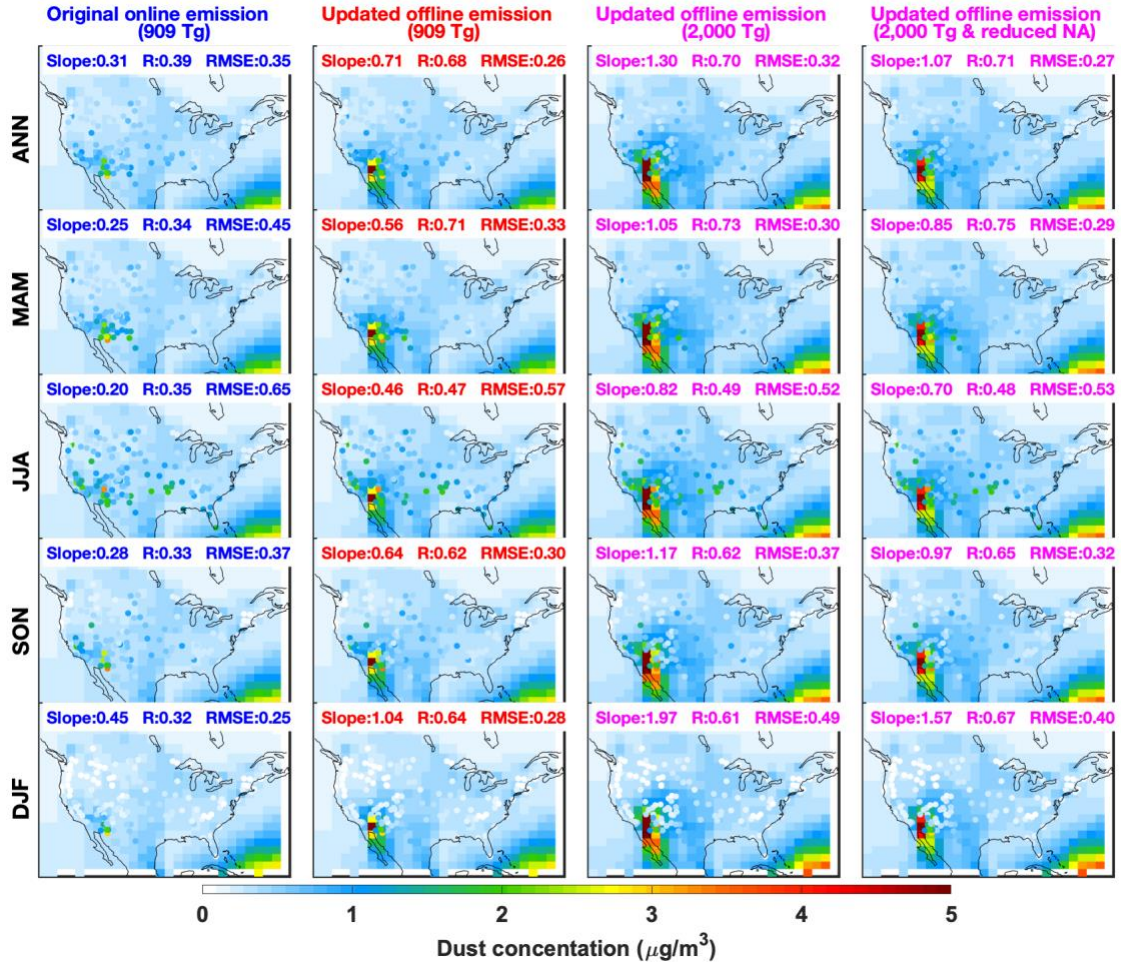


Figure R4. Annual and seasonal mean simulated fine dust concentrations from GEOS-Chem simulations with different dust emissions for 2016, and IMPROVE fine dust measurements, which are shown as filled circles. The right column shows the corresponding scatter plot with root mean square error (E), correlation coefficient(R) and slope (M) calculated with reduced major axis linear regression. The results for the simulation using the original dust emissions are shown in blue (left column); the results for the simulation using updated dust emissions with dust strength of 909 Tg yr<sup>-1</sup> are shown in red (second column); the results for the simulation using updated dust emissions with dust strength of 2,000 Tg yr<sup>-1</sup> are shown in magenta (third column); the right column is the sensitivity simulation with North America dust emission reduced by 30%.

6/ Additional computational time required for calculating dust fluxes in HEMCO when using the offline approach should be presented and discussed.

Response: We added the computational time required for calculating the high resolution offline dust emissions in the main text in line 126 as below:

*“The computational time required for calculating offline dust emission fluxes at 0.25 ° x 0.3125 ° resolution is around 6 hours for one-year of offline dust emissions on a compute node with 32 cores on 2 Intel CPUs at 2.1 GHz.”*

## Anonymous Referee #2:

This work provides a quick and smart way to fix an issue associated with the nonlinear dependency of soil dust emissions on grid resolutions. Dust emissions are known to be a function of fourth or third power of grid-scale wind speeds, which are not a conserved quantity while regridding meteorological data for downscaling or upscaling simulations. As a result, this causes several issues, including not only simulated discrepancy from the observations but also more seriously a breach of mass conservation of soil dust aerosols using the same meteorology but different grid resolutions. Authors developed an offline approach to pre-calculate dust emissions with the finest wind speed data and to use it independent on the model grid resolutions. By doing this, they were able to use consistent dust emissions for simulations with different grid resolutions and also even scale it to better match with observations. I recommend this work for publication at GMD after addressing a few concerns about this work as follows:

**Response:** Thank you for your assessment.

1. Description of soil dust mobilization using the finest wind speed data is clearly written but its application for the coarse model resolutions needs a bit of more elaboration. For example, dust emissions on a finer resolution are simply summed up online while used for coarse model simulations. If this is the case, an instantaneous mixing of dust emission would occur. I guess that this would not be a serious issue for fine-mode dust bins. But, for example, coarse-mode dust aerosols emitted from 0.2 degree grid box could be instantaneously mixed into 2 degree grid box. Any problem with this?

**Response:** It's a common practice for coarse resolution models to represent processes at their resolution. This process fulfills the objective of this work.

2. Following up the first comment above, how do you simulate the dry deposition of dust aerosols, which are also dependent on grid-scale mixing and other micro-scale meteorological parameters. A similar issue could arise if authors use the same gridscale dry deposition calculation especially for coarse mode dust aerosols.

**Response:** The dry deposition of dust includes the effect of gravitational settling and turbulent resistance to the surface. The parameterization of those two effects in GEOS-Chem is represented by the dry deposition velocity induced by those two effects. Dry deposition velocities were calculated for each bin. Those processes are done in the simulation grid. Nonlinear deposition effects are beyond the scope of this work.

We have included the following details in line 146 to elaborate the dry deposition scheme in our model.

*“Dry deposition of dust includes the effects of gravitational settling and turbulent resistance to the surface, which are represented with deposition velocities in the parameterization, implemented into GEOS-Chem by Fairlie et al. (2007).”*

3. I wonder how the model evaluation against AOD observations could properly represent the model capability to simulate dust aerosols and especially dust mobilization. Not only AOD but also Angstrom exponent or other aerosol optical properties would be helpful to give a proper measure of the model performance.

**Response:** Given the paucity of direct dust mass measurements at the global scale, we use AOD close to dust emissions source regions to optimize the AOD simulation. Although we do not have access to appropriate aerosol size or other optical measurements to evaluate our simulation, we conducted other comparisons with measurements of surface fine dust concentration over the US (Figure R4) and dust surface concentration measurements at several independent sites over the globe (Figure R3).

### Anonymous Referee #3:

The authors generate high spatial and temporal resolution mineral dust emissions fields that can be prescribed for use in lower-resolution simulations with the GEOS-Chem model. Online dust emissions are well known to depend on model resolution because of nonlinearity in the governing parameterization. The use of consistent dust emissions across model resolutions overcomes this problem. I disagree with Referee 1 on his/her main point, and agree with Referee 3 on his/hers. The modeler wants to represent the most accurate dust emissions distribution possible irrespective of model resolution, and in particular whether or not they are consistent with the coarse model wind field. Representing high-resolution emissions, even crudely at lower resolution, is much preferred than not representing them at all. Specifically, smoothing of the wind fields at coarser resolution leads to wind speeds falling below the threshold and zero dust emissions in locations that do emit dust. Scaling of global emissions to match those generated at higher resolution leads to unrealistic amplification (hotspots) elsewhere. This is a real problem that the proposed methodology alleviates. The authors make good use of AERONET, MODIS-DB and MAIAC datasets to justify an annual global emission total for the year concerned. The manuscript is well written and mostly clear. I recommend the manuscript be accepted with some clarifications.

Response: Thank you very much for your assessment.

#### 1. Question:

1.1 Please clarify how the high resolution (0.25 deg. x 0.25 deg.) satellite identified dust source function (line 79, 110) is obtained.

Response: The source function S1 provides erodibility factor for sparsely vegetated surface with a potential for accumulated fine sediments. The potential location of accumulated sediments S1 has been determined by comparing the elevation of any 1 x 1 degree grid point with its surrounding hydrological basin using the same equation 1 of Ginoux et al. (2001). The function S1 is then linearly interpolated on a 0.25 degree Cartesian grid and multiplied by the fraction of bare surface within the grid cell. Such surfaces are obtained globally from the classes 8 (bare ground) and 9 (shrubs and bare ground) of the land cover inventory retrieved from the multi-year 8 km AVHRR data (DeFries et al., 2000). It is assumed that 100% of class 8 is bare, while only 20% for class 9. According to the survey by the Chinese Academy of Sciences (CAS, 1998), desertification has increased the bare sandy lands in China. To include these barren lands, we follow the methodology followed by Gong et al. (2003) to use the Chinese Desertification Map (Sunling Gong personal communication) and consider the desertification classes 1 (serious desertification soil), 2 (heavy desertification soil), 3 (current desertification soil) with 80% erodible bare surface, and classes 4 (potential desertification soil) and 5 (low-grade desertification soil) with 60% erodible bare surface.

We added a new section “S2. Description of the updated source function” in the supplemental material as the following:

#### ***“S2. Description of the updated source function***

*The updated source function provides erodibility factor for sparsely vegetated surface with a potential for accumulated fine sediments. The potential location of accumulated sediments has been determined by comparing the elevation of any 1 x 1 degree grid point with its surrounding hydrological basin using the same equation 1 of Ginoux et al. (2001). The updated source function is then linearly interpolated on a 0.25 degree Cartesian grid and multiplied by the fraction of bare surface within the grid cell. Such surfaces are obtained globally from the classes 8 (bare ground) and 9 (shrubs and bare ground) of the land cover inventory retrieved*

*from the multi-year 8 km AVHRR data (Defries et al., 2000). It is assumed that 100% of class 8 is bare, while only 20% for class 9. According to the survey by the Chinese Academy of Sciences (CAS, 1998), desertification has increased the bare sandy lands in China. To include these barren lands, we follow the methodology followed by Gong et al. (2003) to use the Chinese Desertification Map (Sunling Gong personal communication) and consider the desertification classes 1 (serious desertification soil), 2 (heavy desertification soil), 3 (current desertification soil) with 80% erodible bare surface, and classes 4 (potential desertification soil) and 5 (low-grade desertification soil) with 60% erodible bare surface.”*

1.2 Section S1 refers to Ginoux et al (2001) and Zender et al. (2003). However, how are the surface factors S and in particular the Am factors obtained at this higher resolution?

Response: S is the source function. The high resolution version was obtained as described above in the answer 1.1. We did not update Am factors in this study.

1.3 How is the updated source function then applied (presumably interpolated?) for online 2x2.5 deg. simulations? Please clarify.

Response: The updated high resolution dust source function was interpolated to 2x2.5 deg in the online 2x2.5 deg. simulations.

We have modified the text in line 154 as the following to clarify it:

*“The other one is with the updated version of source function, in which the updated fine resolution source function is interpolated to 2° by 2.5° resolution.”*

2. Line 127: sounds like the default emissions would be at the 2 x 2.5 deg. resolution original source function. Please clarify.

Response: The default emission is at the 2x2.5 deg. resolution with the original source function. The modification in the text in line 153 is:

*“The first one is with the original version of dust source function, thereafter noted as original online dust simulation”*

3. Line 154: it is unclear if these 2 simulations are both conducted at 2x2.5 deg. resolution.

Response: The two simulations are both conducted at 2x2.5 deg resolution.

We stated in line 150 as: “We conduct global simulations with GEOS-Chem (version 12.5.0) at a horizontal resolution of 2° by 2.5° for the year 2016.”

#### **Anonymous Referee #4:**

The production of an improved dust emission dataset would be useful for CTMs varying spatial resolution (and idealized simulations in multi-model studies like AeroCom). Generation of high spatial and temporal resolution mineral dust emissions fields for use in lower-resolution simulations is thus a worthwhile product. However, I find the light evaluation of the simulations a concern. Improving the evaluation would increase confidence if the proposed dust emissions are representative at both global and regional levels. For example, only having a single AERONET observation site (and only in spring?) for all of Asia is particularly concerning, especially given issues with satellite retrievals over land. There also appears to be no evaluation of Southern Hemisphere sources. Until a more comprehensive evaluation of the dust atmospheric state is undertaken an evaluation of emissions, and thus the dataset as whole, is difficult to judge.

*Response:* Thank you for your assessment. We have included more evaluations using different types of measurements, including fine dust concentration measurements over the US from the IMPROVE network and a compilation of surface dust concentrations measurements over 12 independent sites over the globe. Please see our responses to the specific comments.

It is probably good to point out that models have a large uncertainty in predicting AOD themselves. Therefore, a reliance on evaluating with only this variable is somewhat questionable. Furthermore, in the Southern Hemisphere satellites revivals are hindered persistent high levels of clouds and that dust activity also tends to occur later in the afternoon after the overpass of polar satellites (e.g., Gassó & Torres, 2019). Comparison to observations of dust concentration and deposition (e.g., Albani et al., 2015), can alleviate the dependency on remote sensing and modelling of one variable. I recommend such an evaluation be included.

*Response:*

We have added model evaluations with measurements of surface dust concentrations.

Firstly, we compare our modeled fine dust surface concentration with the observation from IMPROVE network. As shown in Figure R4, the simulations using the updated offline dust emissions can better represent the observed surface fine dust concentration measurements than the simulation using the original online dust emissions with higher correlations and slopes, annually and seasonally. Scaling the annual dust strength to 2,000 Tg/yr further improved the performance of the model simulation of fine dust concentrations in all seasons except winter. This gives us the same conclusion as the AOD evaluations.

We will add Figure R4 into our main text as Figure 5 and add a new subsection (Sect. 3.3) in the main text in line 250 to describe the results in Figure 5:

#### ***“3.3 Evaluation of the simulations against surface dust concentration measurements***

*We also evaluate our simulations using different dust emissions against measurements of surface dust concentrations. Figure 5 shows the comparison of modeled fine dust surface concentration against the fine dust concentration observation from the IMPROVE network. The simulations using the updated offline dust emissions can better represent the observed surface fine dust concentration measurements than the simulation using the original online dust emissions with higher correlations and slopes across all seasons. Annually, the correlation between the simulation and observation increases from 0.39 to 0.68, and the slope increases from 0.31 to 0.71 when using the updated offline dust emissions with annual dust strength of 909 Tg compared to the simulation using the original online dust emissions. Scaling the annual dust strength to 2,000 Tg/yr marginally improves the performance of the model simulation of fine dust*

concentrations in all seasons except winter, during which the surface fine dust concentrations are overestimated. Given the specificity and density of the dust measurements, and the disconnect of North American dust emissions from the global source, we conduct an additional sensitivity simulation with North American dust emissions reduced by 30%. The right column shows that the annual slope in the resultant simulation versus observations improves to 1.07. Future efforts should focus on better representing the seasonal variation of dust emissions.”

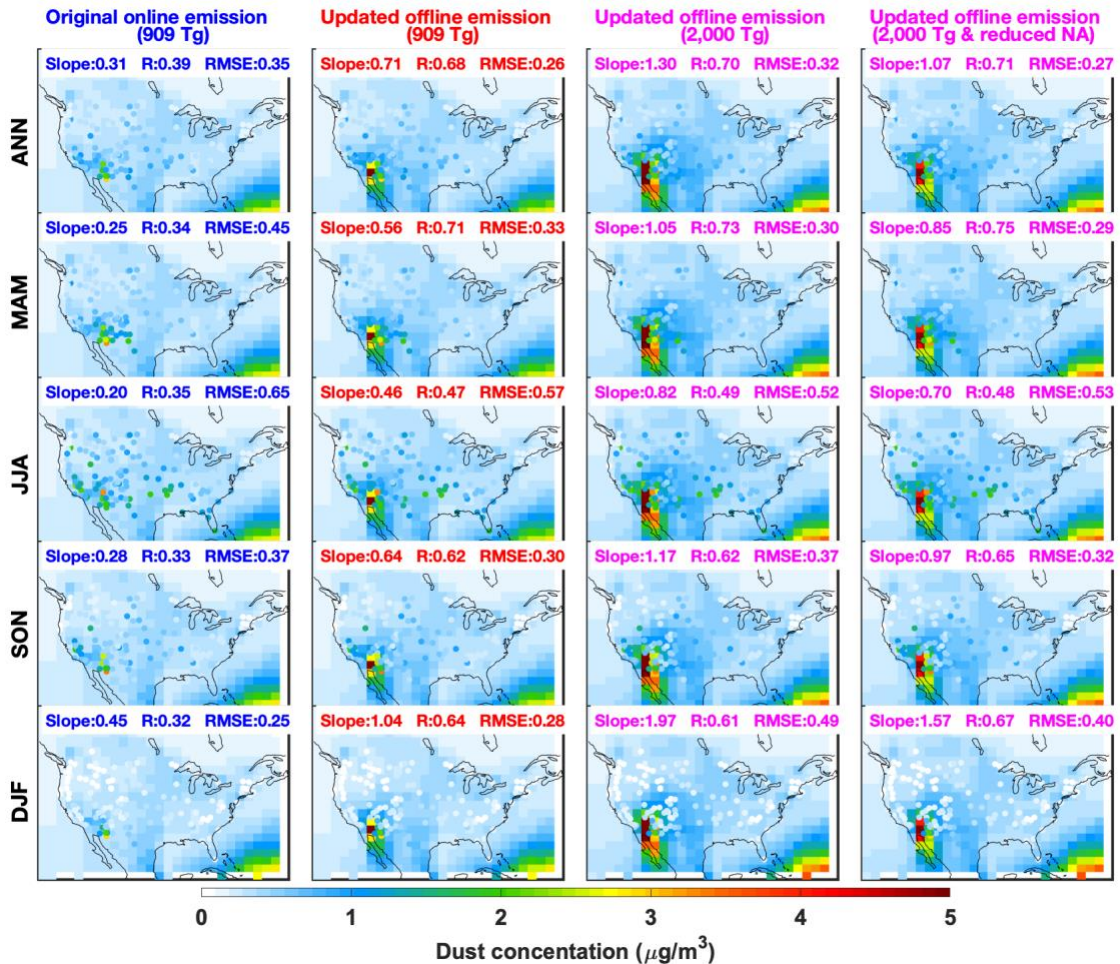


Figure R4. Annual and seasonal mean simulated fine dust concentrations from GEOS-Chem simulations with different dust emissions for 2016, and IMPROVE fine dust measurements, which are shown as filled circles. The right column shows the corresponding scatter plot with root mean square error (E), correlation coefficient(R) and slope (M) calculated with reduced major axis linear regression. The results for the simulation using the original dust emissions are shown in blue (left column); the results for the simulation using updated dust emissions with dust strength of 909 Tg yr<sup>-1</sup> are shown in red (second column); the results for the simulation using updated dust emissions with dust strength of 2,000 Tg yr<sup>-1</sup> are shown in magenta (third column); the right column is the sensitivity simulation with North America dust emission reduced by 30%.

Second, we compare our modeled surface dust concentration with a compilation of surface dust concentrations measurements from 12 independent sites across the globe as shown in Figure R2

(we will include this figure in our supplement text as Figure S1). Figure R3 shows the comparison of seasonal averaged modeled and measured surface dust concentrations. The simulation using the updated offline dust emissions with dust strength of 2,000 Tg yr<sup>1</sup> is closer to the observations at almost all sites.

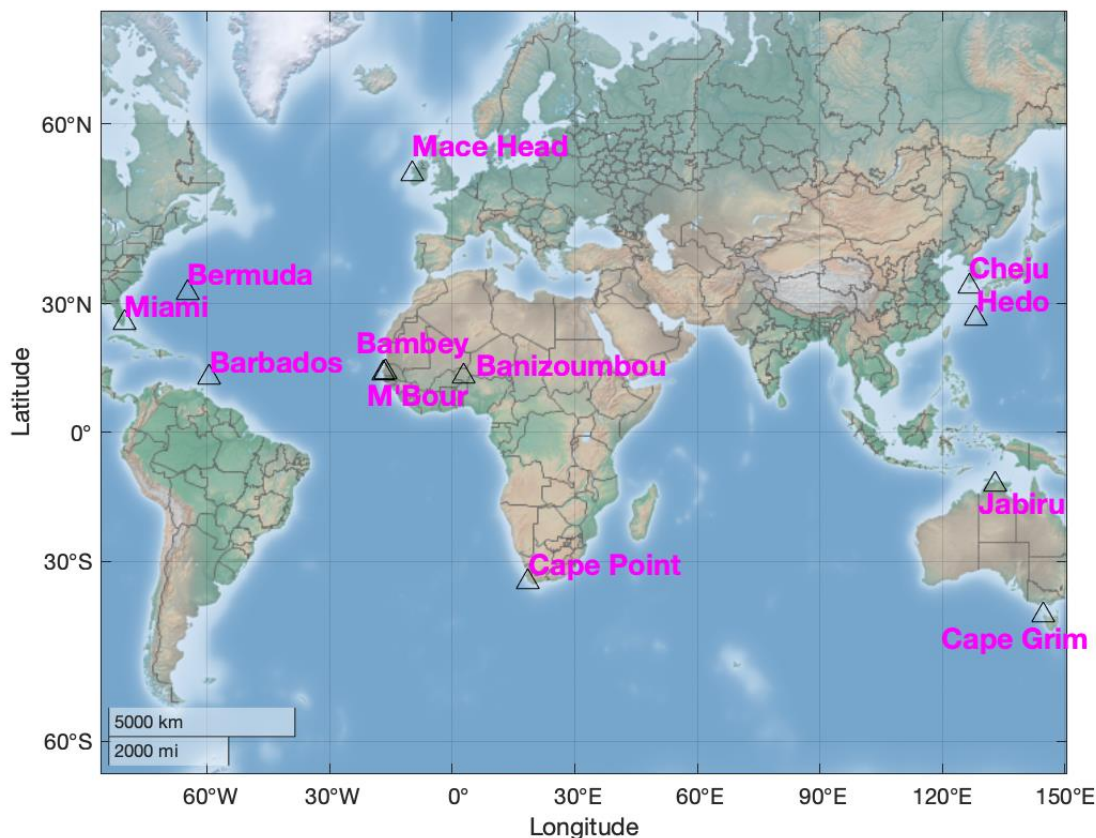


Figure R2. Geolocation of the 12 independent dust surface concentration sites.

We will add Figure R3 into our main text as Figure 6. We add a new paragraph in the main text to describe the results in Figure 6:

*“Figure 6 shows the comparison of seasonal averaged modeled and measured surface dust concentrations from 12 independent sites across the globe. The simulation using the updated offline dust emissions with dust strength of 2,000 Tg yr<sup>1</sup> is more consistent with the observations at almost all sites. The remaining bias at sites distant from source regions, for example sites in the Southern Hemisphere and East Asia, likely reflects remaining uncertainty in representing dust deposition. Further research is needed to address remaining knowledge gaps, such as better representing the dust size distribution and deposition during transport.”*

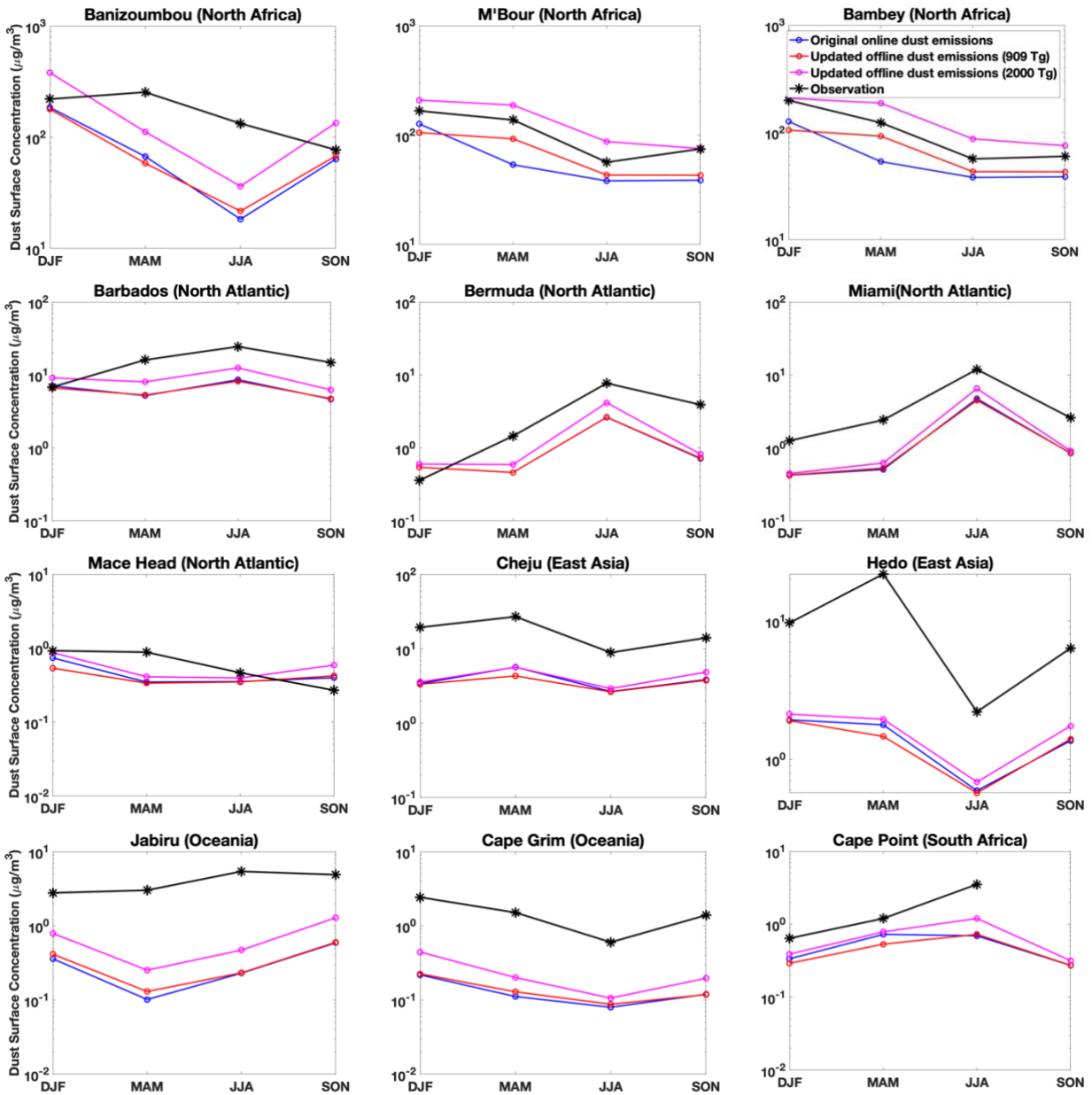


Figure R3. Comparison of modeled and measured seasonal averaged surface dust concentrations at 12 independent globally distributed sites for the years 1981-2000. Nine sites are in the dust belt across Northern hemisphere. The remaining 3 sites are relatively close to the weak dust emission regions in Southern Hemisphere. The results for the simulation using the original dust emissions are shown in blue; the results for the simulation using updated dust emissions with dust strength of 909 Tg yr<sup>-1</sup> are shown in red; the results for the simulation using updated dust emissions with dust strength of 2,000 Tg yr<sup>-1</sup> are shown in magenta. The measurements are in black.

We updated the section 2.1, description of observations, in the main text by adding the descriptions of IMPROVE fine dust observations and the compilation of independent surface dust concentrations measurements in line 99:

*“We use ground-based surface fine dust concentration measurements over the US from the Interagency Monitoring of Protected Visual Environments (IMPROVE, <http://views.cira.colostate.edu/fed/DataWizard/>) network. The IMPROVE network provided 24-hr average fine dust concentrations data every third day over the national parks in the United States. We also include a climatology of dust surface concentrations measurements over 1981-2000 from 27 independent dust measurement sites over the globe (Kok et al. 2020). We use those sites (12 in total) (Figure S1) that either in the dust belt across Northern Hemisphere or sites relatively close to the weak emission regions in the Southern Hemisphere to evaluate our dust simulation”*

The explanation for the approximate doubling of emissions in the optimal simulation appears to be to better match North African dust sources, but is the optimization not best served if undertaken regionally? For example, as D. A. Ridley is a co-author a regional AOD evaluation based on (Ridley et al., 2016) should be possible. An optimal estimation of the regional source strengths is particularly important given the goal is to prove a dataset for the community where other dust regions are important contributors to regional climate. E.g., within the Southern Hemisphere in providing IN or dusts role in marine biogeochemical cycles.

Response: Interesting idea. We add a regional optimization for North America where sufficient measurements exist to optimize the regional source (the last column in Figure R4). This idea should be developed in further research. Our current work is mostly about to introduce this offline dust emission capability to ease the nonlinear dependence of dust emission parameterizations upon model resolutions when using online dust emissions.

As significant amounts of dust mass occur above 6 $\mu$ m (Adebiyi & Kok, 2020; Ryder et al., 2019), how does this impact results here and what are the impacts for generating a dataset for other CTMs given the size bins and cut off here?

Response: This is a very good question. As Adebiyi & Kok (2020) concluded, most current models missed the coarse dust particles (diameters beyond 5 microns). So does GEOS-Chem, the model in this study. Since we are optimizing the total dust loading by using AOD measurements, the missing of coarse dust will lead to an underestimation of the total dust emission, which exists large uncertainty in current dust emission parameterizations. However, this is more of a dust size distribution issue. It will be improved with the advanced modeling development of the dust size distribution.

As for the impacts for other CTMs, it would be similar to the impacts on GEOS-Chem, because most other CTMs also missed the coarse dust with a similar dust size cutoff. The future studies would implement coarse dust and more realistic dust size distributions in all CTMs.

Minor Comments: L103: Dust entrainment and deposition

Response: Corrected.

L106: Why is a fixed global value of clay fraction used when datasets are readily available giving the regional fraction. E.g., (Journet et al., 2014)

Response: Firstly, previous studies using the same dust mobilization scheme (DEAD) as our work have indicated that DEAD is overly sensitive to clay fraction (Zender et al., 2003) and using a global map of clay fraction does not improve the dust simulation in a global scale (Ridley et al., 2012) (see figure 11 in this reference). Second, the focus of our work is to develop the offline dust emission method to alleviate the nonlinear dependence of dust emission parameterizations upon model resolutions. So, we would like to keep as many parameters the same as the original online dust simulation as possible for the offline dust emission calculation. All in all, we use a global fixed value of clay fraction in our dust mobilization scheme as suggested by Zender et al. (2003) and Ridley et al. (2012). Implementing a clay fraction map would be an interesting research topic for future studies.

L119: Define HEMCO?

Response: We have modified our text in line 119 as the following:

*“calculate hourly emissions using the Harmonized Emissions Component (HEMCO) module described below.”*

Refs:

- Adebisi, A. A., & Kok, J. F. (2020). Climate models miss most of the coarse dust in the atmosphere. *Science Advances*, 6(15), 1–10. <https://doi.org/10.1126/sciadv.aaz9507>
- Albani, S., Mahowald, N. M., Winckler, G., Anderson, R. F., Bradtmiller, L. I., Delmonte, B., et al. (2015). Twelve thousand years of dust: the Holocene global dust cycle constrained by natural archives. *Climate of the Past*, 11(6), 869–2015. <https://doi.org/10.5194/cp-11-869-2015>
- Gassó, S., & Torres, O. (2019). Temporal Characterization of Dust Activity in the Central Patagonia Desert (Years 1964–2017). *Journal of Geophysical Research: Atmospheres*, 124(6), 3417–3434. <https://doi.org/10.1029/2018JD030209>
- Journet, E., Balkanski, Y., & Harrison, S. P. (2014). A new data set of soil mineralogy for dust-cycle modeling. *Atmospheric Chemistry and Physics*, 14(8), 3801–3816. <https://doi.org/10.5194/acp-14-3801-2014>
- Ridley, D. A., Heald, C. L., Kok, J. F., & Zhao, C. (2016). An observationally constrained estimate of global dust aerosol optical depth. *Atmospheric Chemistry and Physics*, 16(23), 15097–15117. <https://doi.org/10.5194/acp-16-15097-2016>
- Ryder, C. L., Highwood, E. J., Walser, A., Seibert, P., Philipp, A., & Weinzierl, B. (2019). Coarse and giant particles are ubiquitous in Saharan dust export regions and are radiatively significant over the Sahara. *Atmospheric Chemistry and Physics*, 19(24), 15353–15376. <https://doi.org/10.5194/acp-19-15353-2019>

## References for our responses:

- Bindle, L., Martin, R. V., Cooper, M. J., Lundgren, E. W., Eastham, S. D., Auer, B. M., Clune, T. L., Weng, H., Lin, J., Murray, L. T., Meng, J., Keller, C. A., Pawson, S., and Jacob, D. J.: Grid-Stretching Capability for the GEOS-Chem 13.0.0 Atmospheric Chemistry Model, 1–21, <https://doi.org/10.5194/gmd-2020-398>, 2020.
- Chinese Academy of Sciences, Chinese Desertification Map, Resource and Environment Database, Beijing, 1998.
- Defries, R. S., Hansen, M. C., and Townshend, J. R. G.: Global continuous fields of vegetation characteristics: A linear mixture model applied to multi-year 8 km AVHRR data, 21, 1389–1414, <https://doi.org/10.1080/014311600210236>, 2000.
- Eastham, S. D., Long, M. S., Keller, C. A., Lundgren, E., Yantosca, R. M., Zhuang, J., Li, C., Lee, C. J., Yannetti, M., Auer, B. M., Clune, T. L., Kouatchou, J., Putman, W. M., Thompson, M. A., Trayanov, A. L., Molod, A. M., Martin, R. V., and Jacob, D. J.: GEOS-Chem High Performance (GCHP v11-02c): a next-generation implementation of the GEOS-Chem chemical transport model for massively parallel applications, 11, 2941–2953, <https://doi.org/10.5194/gmd-11-2941-2018>, 2018.
- Fairlie, T. D., Jacob, D. J., and Park, R. J.: The impact of transpacific transport of mineral dust in the United States, *Atmospheric Environment*, 41, 1251–1266, <https://doi.org/10.1016/j.atmosenv.2006.09.048>, 2007.
- Ginoux, P., Chin, M., Tegen, I., Prospero, J. M., Holben, B., Dubovik, O., and Lin, S.-J.: Sources and distributions of dust aerosols simulated with the GOCART model, 106, 20255–20273, <https://doi.org/10.1029/2000JD000053>, 2001.
- Gong, S. L., Zhang, X. Y., Zhao, T. L., McKendry, I. G., Jaffe, D. A., and Lu, N. M.: Characterization of soil dust aerosol in China and its transport and distribution during 2001 ACE-Asia: 2. Model simulation and validation, 108, <https://doi.org/10.1029/2002JD002633>, 2003.
- Kok, J. F., Adebisi, A. A., Albani, S., Balkanski, Y., Checa-Garcia, R., Chin, M., Colarco, P. R., Hamilton, D. S., Huang, Y., Ito, A., Klose, M., Leung, D. M., Li, L., Mahowald, N. M., Miller, R. L., Obiso, V., Pérez García-Pando, C., Rocha-Lima, A., Wan, J. S., and Whicker, C. A.: Improved representation of the global dust cycle using observational constraints on dust properties and abundance, 1–45, <https://doi.org/10.5194/acp-2020-1131>, 2020.
- Ridley, D. A., Heald, C. L., and Ford, B.: North African dust export and deposition: A satellite and model perspective, *Journal of Geophysical Research: Atmospheres*, 117, <https://doi.org/10.1029/2011JD016794>, 2012.
- Zender, C. S., Bian, H., and Newman, D.: Mineral Dust Entrainment and Deposition (DEAD) model: Description and 1990s dust climatology, 108, <https://doi.org/10.1029/2002JD002775>, 2003.

# Grid-independent High Resolution Dust Emissions (v1.0) for Chemical Transport Models: Application to GEOS-Chem (~~version~~ 12.5.0)

Jun Meng<sup>1,2</sup>, Randall V. Martin<sup>2,1,3</sup>, Paul Ginoux<sup>4</sup>, Melanie Hammer<sup>2,1</sup>, Melissa P. Sulprizio<sup>5</sup>,

5 David A. Ridley<sup>6</sup>, Aaron van Donkelaar<sup>1,2</sup>

<sup>1</sup>Department of Physics and Atmospheric Science, Dalhousie University, Halifax, Nova Scotia, B3H 4R2, Canada

<sup>2</sup> Department of Energy, Environmental & Chemical Engineering, Washington University in St. Louis, St. Louis, Missouri 63130, United States

10 <sup>3</sup>Smithsonian Astrophysical Observatory, Harvard-Smithsonian Center for Astrophysics, Cambridge, MA 02138, USA

<sup>4</sup>NOAA Geophysical Fluid Dynamics Laboratory, Princeton, New Jersey 08540, USA

<sup>5</sup>School of Engineering and Applied Science, Harvard University, Cambridge, MA 02138, USA

<sup>6</sup>California Environmental Protection Agency, Sacramento, CA 95814, USA

15

*Correspondence to:* Jun Meng ([jun.meng@ucla.edu](mailto:jun.meng@ucla.edu)~~dal.ca~~)

**Abstract.** The nonlinear dependence of the dust saltation process on wind speed poses a challenge for models of varying resolutions. This challenge is of particular relevance for the next generation of chemical transport models with nimble capability for multiple resolutions. We develop and apply a method to harmonize dust emissions across simulations of different resolutions by generating offline grid independent dust emissions driven by native high resolution meteorological fields. We implement into the GEOS-Chem chemical transport model a high resolution dust source function to generate updated offline dust emissions. These updated offline dust emissions based on high resolution meteorological fields strengthen dust emissions over relatively weak dust source regions~~These updated offline dust emissions based on high resolution meteorological fields can better resolve weak dust source regions~~, such as in southern South America, southern Africa and the southwestern United States. Identification of an appropriate dust emission strength is facilitated by the resolution independence of offline emissions. We find that the performance of simulated aerosol optical depth (AOD) versus measurements from the AERONET network and satellite remote sensing improves significantly when using the updated offline dust emissions with the total global annual dust emission strength of 2,000 Tg yr<sup>-1</sup> rather than the standard online emissions in GEOS-Chem. The offline high resolution dust emissions are easily implemented in chemical transport models. The source code is and available online through GitHub: <https://github.com/Jun-Meng/geos-chem/tree/v11-01-Patches-UniCF-vegetation>~~The global offline high-resolution dust emission inventory are publicly is freely available e (see Code and Data Availability section).~~

## 1 Introduction

Mineral dust, as one of the most important natural aerosols in the atmosphere, has significant impacts on weather and climate by absorbing and scattering solar radiation (Bergin et al., 2017; Kosmopoulos et al., 2017), on atmospheric chemistry by providing surfaces for heterogeneous reaction of trace gases (Chen et al., 2011; Tang et al., 2017), on the biosphere by fertilizing the tropical forest (Bristow et al., 2010; Yu et al., 2015), and on human health by increasing surface fine particulate matter (PM<sub>2.5</sub>) concentrations (De Longueville et al., 2010; Fairlie et al., 2007; Zhang et al., 2013). Dust emissions are primarily controlled by surface wind speed to the third or fourth power, vegetation cover and soil water content. The principal mechanism for natural dust emissions is saltation bombardment (Gillette and Passi, 1988; Shao et al., 1993), in which sand-sized particles creep forward and initiate the suspension of smaller dust particles when the surface wind exceeds a threshold. The nonlinear dependence of dust emissions on meteorology ~~ity of this process~~ introduces an artificial dependence of simulations upon model resolution (Ridley et al., 2013). For example, dust emissions in most numerical models are parameterized with an empirical method (e.g. Ginoux et al., 2001; Zender et al., 2003), which requires a critical wind threshold to emit dust particles. Smoothing meteorological fields to coarse resolution can lead to wind speeds falling below the emission threshold in regions that do emit dust. Methods are needed to address the artificial dependence of simulations upon model resolution that arises from nonlinearity in dust emissions.

Addressing this nonlinearity is especially important for the next generation of chemistry transport models that is emerging with nimble capability for a variety of resolutions at the

global scale. For example, the high performance version of GEOS-Chem (GCHP) (Eastham et al., 2018) currently offers simulation resolutions that vary by over a factor of 100 from C24 (~  
65  $4^\circ \times 45^\circ$ ) to C360 ( $\sim 0.25^\circ \times 0.25^\circ$ ), with progress toward even finer resolution and toward a  
variable stretched grid capability (Bindle et al., 2020). Resolution-dependent mineral dust  
emissions would vary by a factor of 3 from C360 to C24, ~~and inhibit interpretation~~ (Ridley et al.,  
2013). Such large resolution-dependent biases would undermine applications of CTMs to assess  
dust effects, and would lead to large within-simulation inconsistency for stretched grid  
70 simulations that can span the entire resolution range simultaneously. Grid-independent high  
resolution dust emissions offer a potential solution to this ~~concern~~ issue.

An important capability in global dust evaluation is ground-based and satellite remote  
sensing. The Aerosol Robotic Network (AERONET), a global ground-based remote sensing  
aerosol monitoring network of Sun photometers (Holben et al., 1998), has been widely used to  
75 evaluate dust simulations. Satellite remote sensing provides additional crucial information  
across arid regions where in-situ observations are sparse (Hsu et al., 2013). Satellite aerosol  
retrievals have been used extensively in previous studies to either evaluate the dust simulation  
(Ridley et al., 2012, 2016) or constrain the dust emission budget (Zender et al., 2004). Satellite  
aerosol products have been used to identify dust sources worldwide (Ginoux et al., 2012;  
80 Schepanski et al., 2012; Yu et al., 2018), especially for small-scale sources (Gillette, 1999).

The objective of this study is to develop a method to mitigate the large inconsistency of  
total dust emissions across different resolutions of simulations by generating and archiving ~~an~~  
offline dust emissions using native high resolution meteorological fields. We apply this method  
to the GEOS-Chem chemical transport model. As part of this effort, we implement an updated

85 high resolution satellite-identified dust source function into the dust mobilization module of  
GEOS-Chem to better represent the spatial structure of dust sources. We apply this new  
capability to assess the source strength that best represents observations.

## 2 Materials and Methods

### 90 2.1 Description of Observations

We use both ground-based and satellite observations to evaluate our GEOS-Chem simulations.  
AERONET is a global ground-based remote sensing aerosol monitoring network of sun  
photometers with direct sun measurements every 15 minutes (Holben et al., 1998). We use  
Level 2.0 Version 3 data that has improved cloud screening algorithms (Giles et al., 2019).

95 Aerosol optical depth (AOD) at 550 nm is interpolated based on the local Aangstrom exponent  
at the 440 nm and 670 nm channels.

Twin Moderate-Resolution Imaging Spectroradiometer (MODIS) instruments aboard  
both on the Terra and Aqua NASA satellite platforms ~~and~~ provide near daily measurements  
globally. We use the AOD at 550 nm retrieved from Collection 6.1 (C6) of MODIS product (Sayer  
100 et al., 2014). We use AOD from the Deep Blue (DB) retrieval algorithm (Hsu et al., 2013; Sayer et  
al., 2014) designed for bright surfaces, and the Multi-Angle Implementation of Atmospheric  
Correction (MAIAC) algorithm (Lyapustin et al., 2018), which provides global AOD retrieved  
from MODIS C6 radiances at a resolution of 1 km. The MAIAC AOD used in this study is  
interpolated to the AOD value at 550 nm.

105 We use ground-based surface fine dust concentration measurements over the US from  
the Interagency Monitoring of Protected Visual Environments (IMPROVE,

<http://views.cira.colostate.edu/fed/DataWizard/>) network. The IMPROVE network provides 24-hr average fine dust concentrations data every third day over the national parks in the United States. We also include a climatology of dust surface concentrations measurements over 1981-2000 from independent dust measurement sites over the globe (Kok et al. 2020). We use those sites (12 in total) (Figure S1) that either in the dust belt across Northern Hemisphere or sites relatively close to the weak emission regions in the Southern Hemisphere to evaluate our dust simulation. (Kok et al., 2020)

We compare the simulated ~~fine~~-AOD and dust concentrations with measurements using reduced major axis linear regression. We report root mean square error (E), correlation (R) and slope (M).

## 2.2 Dust mobilization module

We use the dust ~~en~~detrainment and deposition (DEAD) scheme (Zender et al., 2003) in the GEOS-Chem model to calculate dust emissions. The saltation process is dependent on the critical threshold wind speed, which is determined by surface roughness, soil type and soil moisture. ~~We use a fixed soil clay fraction of 0.2 as suggested in Zender et al. (2003).~~ Dust aerosol is transported in four size bins (0.1-1.0, 1.0-1.8, 1.8-3.0, and 3.0-6.0  $\mu\text{m}$  radius).

Detailed description of the dust emission parameterization is in Sect. S1 of the supplemental material.

The fractional area of land with erodible dust is represented by a source function. The dust source function used in the dust emission module plays an important role in determining the spatial distribution of dust emissions. The standard GEOS-Chem model (version 12.5.0) uses

a source function at  $2^\circ \times 2.5^\circ$  resolution from Ginoux et al. (2001) as implemented by Fairlie et al. (2007). We implement an updated high resolution version of the dust source function in this study at  $0.25^\circ \times 0.25^\circ$  resolution (Sect. S2). Figure S24 shows a map of the original and updated version of the dust source function. The updated source function exhibits more spatially resolved information due to its finer spatial resolution resulting in a higher fraction of erodible dust over in the eastern Arabian Peninsula, the Bodélé depression, and the central Asian deserts. The dust module dynamically applies this source function, together with information on soil moisture, vegetation, and land use to calculate hourly emissions using the [Harmonized Emissions Component \(-HEMCO\)](#) module described below.

### 2.3 Offline dust emissions at the native meteorological resolution

HEMCO (Keller et al., 2014) is a stand-alone software module for computing emissions in global atmospheric models. We run the HEMCO standalone version using native meteorological resolution ( $0.25^\circ \times 0.3125^\circ$ ) data [for wind speed, soil moisture, vegetation, and land use](#) to archive the offline dust emissions at the same resolution as the meteorological data. [The computational time required for calculating offline dust emission fluxes at  \$0.25^\circ \times 0.3125^\circ\$  resolution is around 6 hours for one-year of offline dust emissions on a compute node with 32 cores on 2 Intel CPUs at 2.1 GHz. \(Graham—CC-Dee, 2021\)](#) In this study, we generate two offline dust emission datasets at  $0.25^\circ \times 0.3125^\circ$  resolution. One, referred to as the default offline dust emissions, uses the existing dust source function in the [GEOS-Chem](#) dust module; the other, referred to as the updated offline dust emissions, uses the updated dust source function implemented here. Both datasets are at the hourly resolution of the parent meteorological

fields. The archived native resolution offline dust emissions can be conservatively regridded to coarser resolution for consistent input to an input emission inventory for chemical transport models with scalable dust source strengths at multiple resolutions. We use the GEOS-Chem model to evaluate the dust simulations and the emission strength.

155

#### 2.4 GEOS-Chem chemical transport model and simulation configurations

GEOS-Chem (The International GEOS-Chem User Community, 2019) is a three-dimensional chemical transport model driven by assimilated meteorological data from the Goddard Earth Observation System (GEOS) of the NASA Global Modelling and Assimilation Office (GMAO). The GEOS-Chem aerosol simulation includes the sulfate-nitrate-ammonium (SNA) aerosol system (Fountoukis and Nenes, 2007; Park et al., 2004), carbonaceous aerosol (Hammer et al., 2016; Park et al., 2003; Wang et al., 2014), secondary organic aerosols (Marais et al., 2016; Pye et al., 2010), sea salt (Jaeglé et al., 2011) and mineral dust (Fairlie et al., 2007) with updates to aerosol size distribution (Ridley et al., 2012; Zhang et al., 2013). Aerosol optical properties are based on the Global Aerosol Data Set (GADS) as implemented by Martin et al. (2003) for externally mixed aerosols as a function of local relative humidity with updates based on measurements (Drury et al., 2010; Latimer and Martin, 2019). Wet deposition of dust, including the processes of scavenging from convections and large scale precipitations, is presented by the scheme developed by follows Liu et al. (2001). Dry deposition of dust includes the effects of gravitational settling (Seinfeld and Pandis, 1998) and turbulent resistance to the surface, (Zhang et al., 2001), which are represented with deposition velocities in the parameterization, implemented into GEOS-Chem by Fairlie et al. (2007).

170

The original GEOS-Chem simulation used online dust emissions by coupling the dust mobilization module online. We develop the capability to use offline dust emissions based on the archived fields described in Sect. 2.3. We conduct global simulations with GEOS-Chem (version 12.5.0) at a horizontal resolution of  $2^\circ$  by  $2.5^\circ$  for the year 2016. Simulations using the online and offline dust emissions are conducted to evaluate the offline dust emissions. We conduct two simulations using online dust emissions with different dust source functions. The first is with the original version of dust source function, hereafter noted as the original online dust simulation. The other ~~one~~ is with the updated version of source function, in which the updated fine resolution source function is interpolated to  $2^\circ$  by  $2.5^\circ$  resolution. The annual total emissions for the online dust emissions are at the original value of  $909 \text{ Tg yr}^{-1}$ . We conduct another ~~two~~ four sets of simulations using offline dust emissions. The first uses the default offline dust emissions with ~~the~~ annual total dust emission of  $909 \text{ Tg yr}^{-1}$ . The remaining second ~~uses~~ use the updated offline dust emissions with the annual total dust emission scaled to 1,500, 2,000 and 2,500  $\text{Tg yr}^{-1}$ , which ~~are~~ is in the range of the current dust emission estimates of over  $426 - 2,726 \text{ Tg yr}^{-1}$  (Huneeus et al., 2011). We focus on the simulation with  $2,000 \text{ Tg yr}^{-1}$  which and better represents observations as will be shown below.

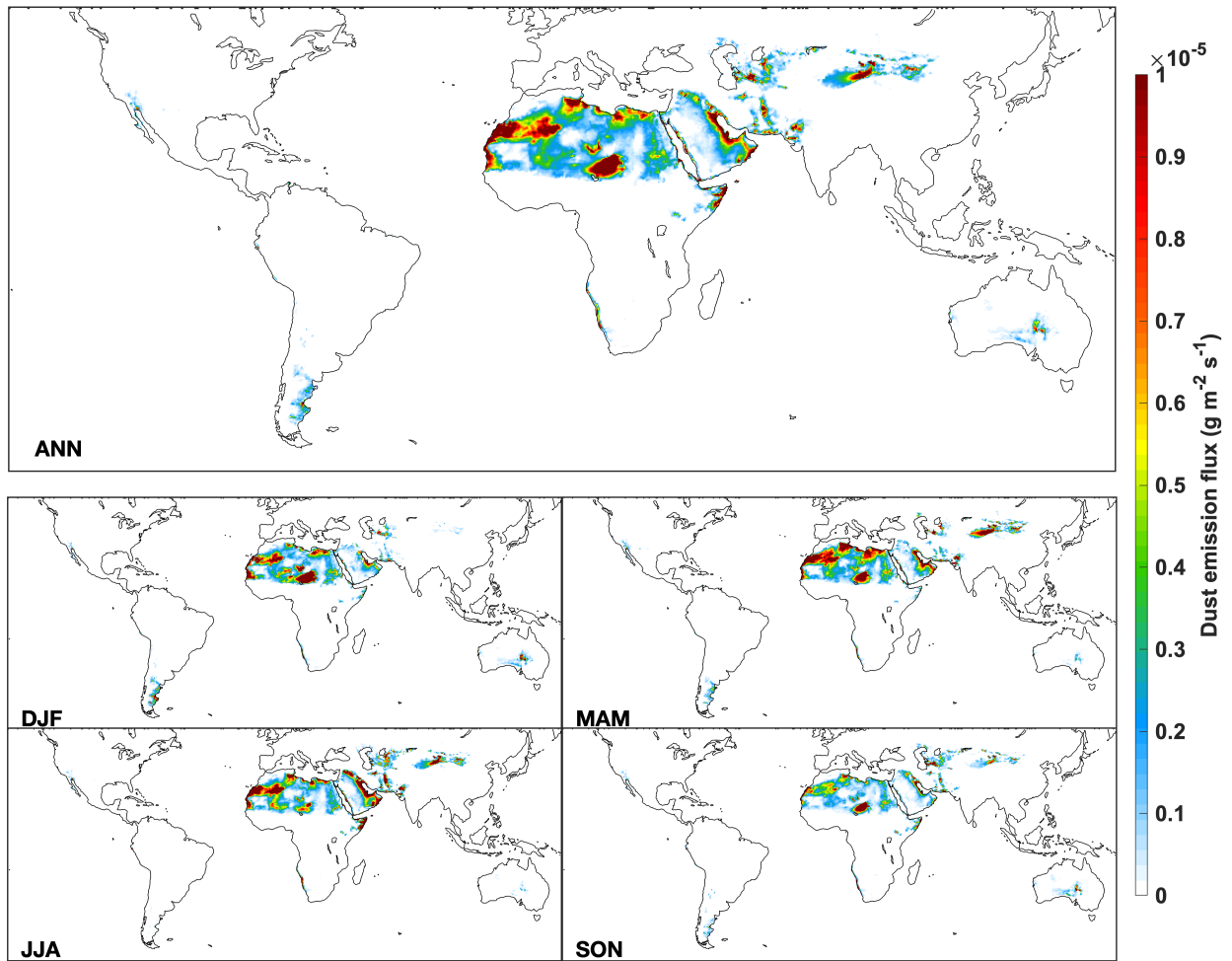
## 190 **3 Results and Discussion**

### **3.1 Spatial and seasonal variation of the offline dust emissions**

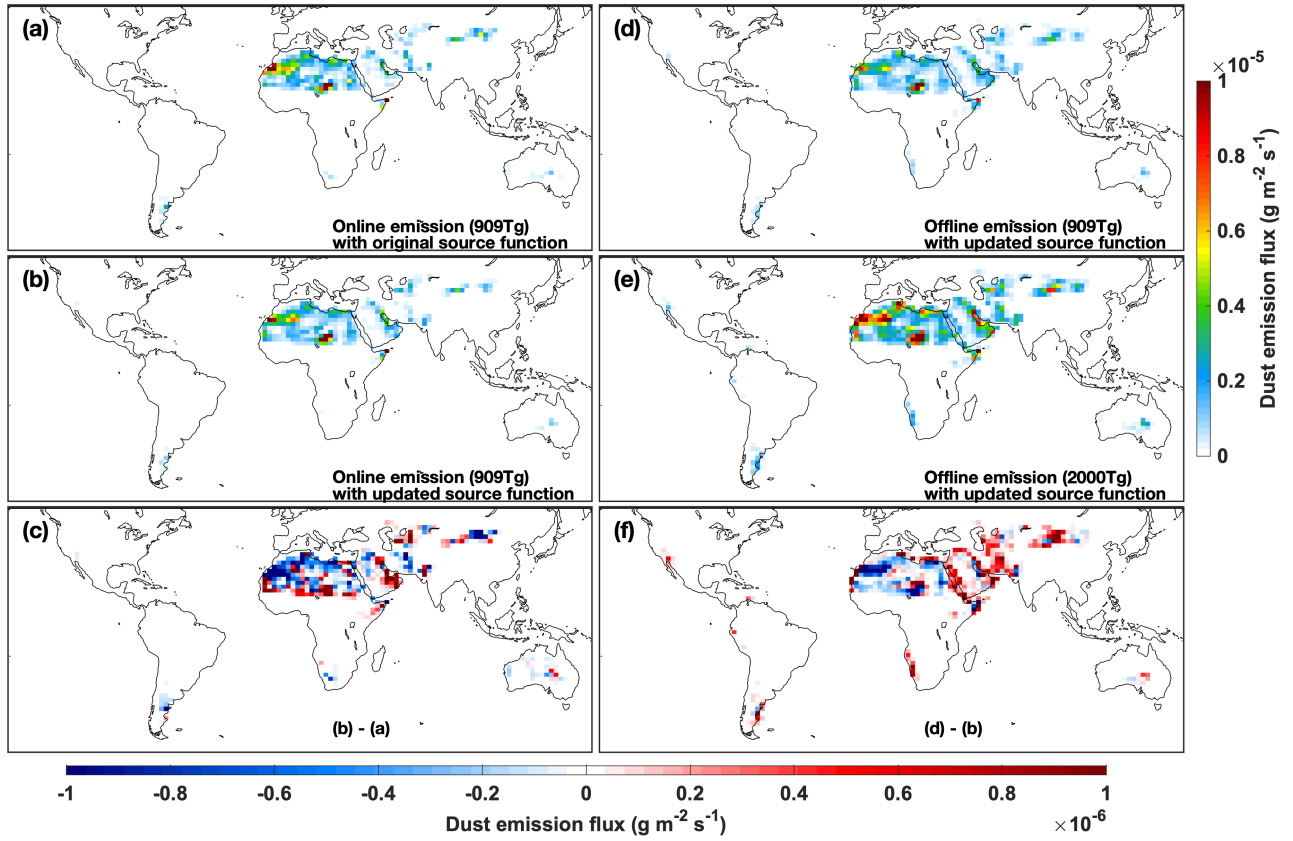
Figure 1 shows the spatial distribution of the annual and seasonal dust emission flux rate for the updated offline dust emissions. The annual dust emission flux rate is high over major deserts, such as the northwestern Sahara, the Bodélé Depression in northern Chad, eastern

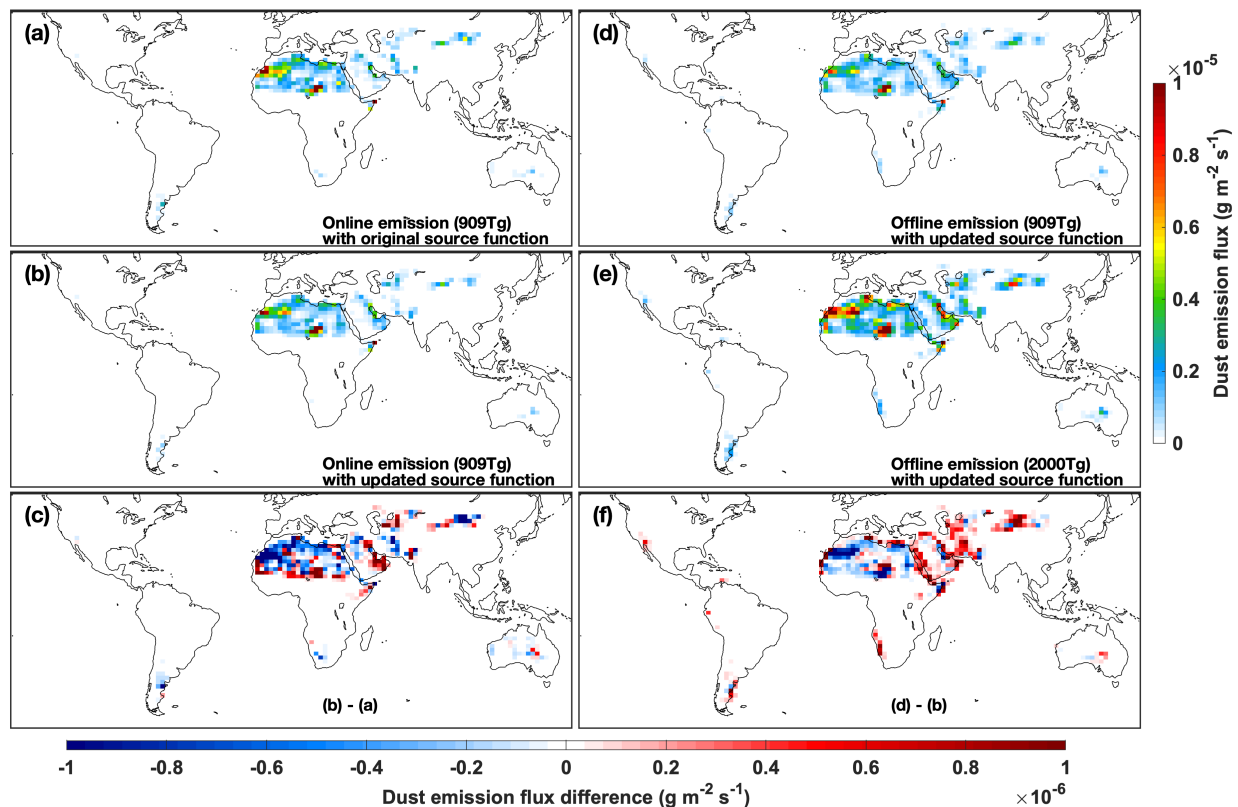
195 Arabian Peninsula and central Asian Taklimakan and Gobi deserts. There are also hotspots of dust emission flux rate over relatively smaller deserts, such as the Mojave Desert of the southwestern United States, the Atacama desert of southern South America, the Kalahari desert on the west coast of southern Africa and the deserts in central Australia. Those features reflect the fine resolution of the updated dust source function and of the offline dust emissions.

200 Seasonally, the dust emission flux rate resembles the annual distribution, however, with a lower dust emission flux rate over the Bodélé Depression in northern Chad in summer and higher dust emission flux rate over the Middle East and central Asian deserts in spring and summer.



205 Figure 14. Annual and seasonal mean dust emission flux rate for the offline high resolution dust emissions with updated dust source function and updated annual total dust emission of 2,000 Tg.





210

Figure 22. Annual mean dust emission flux rate for 2016. (a), The original online dust emissions with original dust source function and annual total dust emissions of 909 Tg. (b), Online dust emissions with updated dust source function. (c), Difference of flux rate between online dust emissions using original and updated dust source functions. (d), Offline dust emissions with updated dust source function. (e), Offline dust emissions with updated dust source function and updated annual total dust emissions of 2,000 Tg. (f), Difference of flux rate between offline and online dust emissions. The online dust emissions are in  $2^\circ \times 2.5^\circ$  resolution. The offline dust emissions shown in (b), (d), (f) are regridded from  $0.25^\circ \times 0.3125^\circ$  resolution to  $2^\circ \times 2.5^\circ$  for comparison with online dust emissions.

215

Figure 2 shows the spatial distribution of the annual dust emission flux rate for the online and offline dust emissions with the original and updated dust source functions with original and updated global total dust source strengths. All simulations exhibit high dust emission flux rates over major desert regions, such as the Sahara, Middle East and Central Asian deserts, with local enhancements over the western Sahara and northern Chad. The simulation with the updated source function exhibits stronger emissions in the Sahara and Persian Gulf

220

regions (Fig. 2c). The difference between the online and offline dust emissions, shown in Fig. 2f,

225 can be considered the error in the online approach arising from coarse resolution

meteorological fields. ~~Indicates that~~ the offline dust emissions based on native resolution

meteorological fields have lower dust emission flux rates over northwest Africa, but higher dust

emission flux rates over the Middle East and Central Asia. Higher annual dust emission flux

rates over the southwestern United States, southern South America, the west coast of southern

230 Africa and central Australia in the offline dust emissions reflect that the native resolution offline

dust emissions are strengthened over relatively weaker dust emission regions. Generally,

coastal and minor desert regions emit more dust when calculating emissions at the native

meteorological resolution.

Figures S32–S65 show the seasonal variations of dust emission flux rates for online and

235 offline emissions. The offline dust emissions have lower emission flux rates than the online dust

emissions during spring (March, April and May) (MAM) and winter (December, January and

February) (DJF) over the Sahara Desert. The offline dust emission flux rate is higher than the

online dust emission flux rate over the Middle East and Central Asian deserts during spring and

summer (June, July and August) (JJA). Emission flux rates are low over Central Asian deserts

240 during winter. The strengthening of offline dust emissions over weaker dust emitting regions

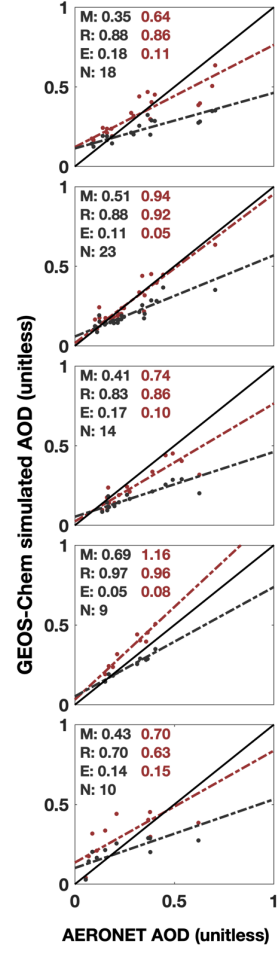
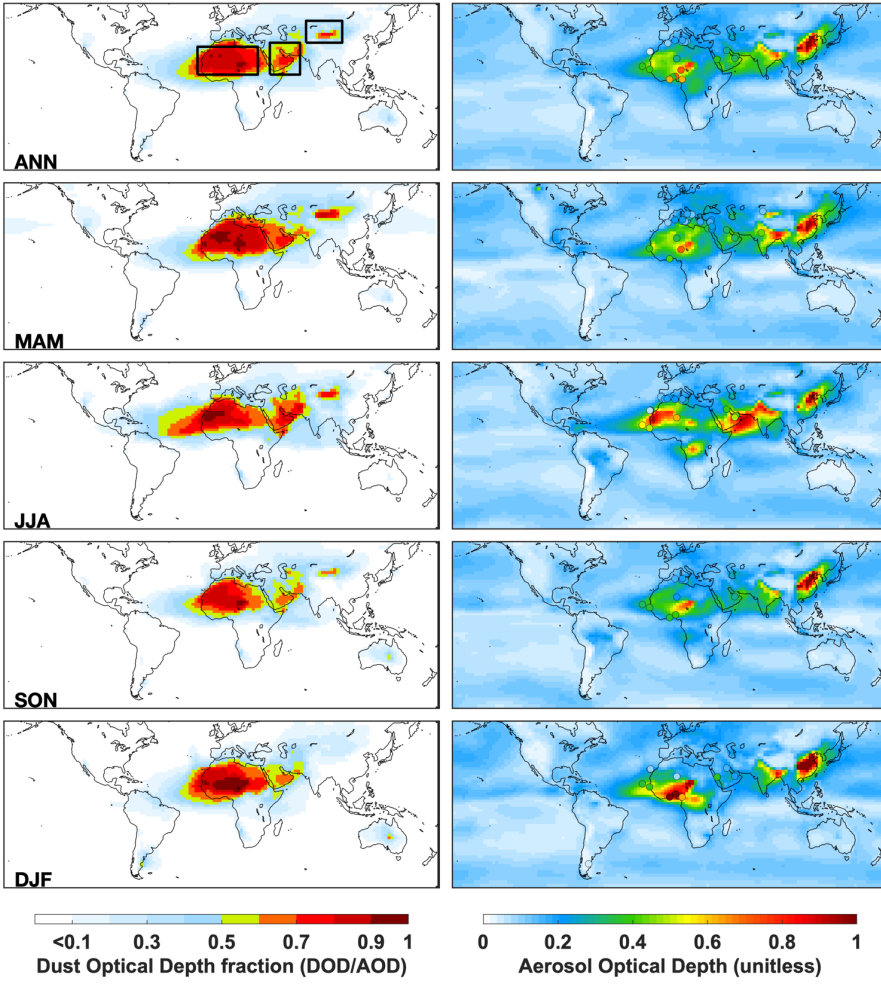
persists throughout all seasons.

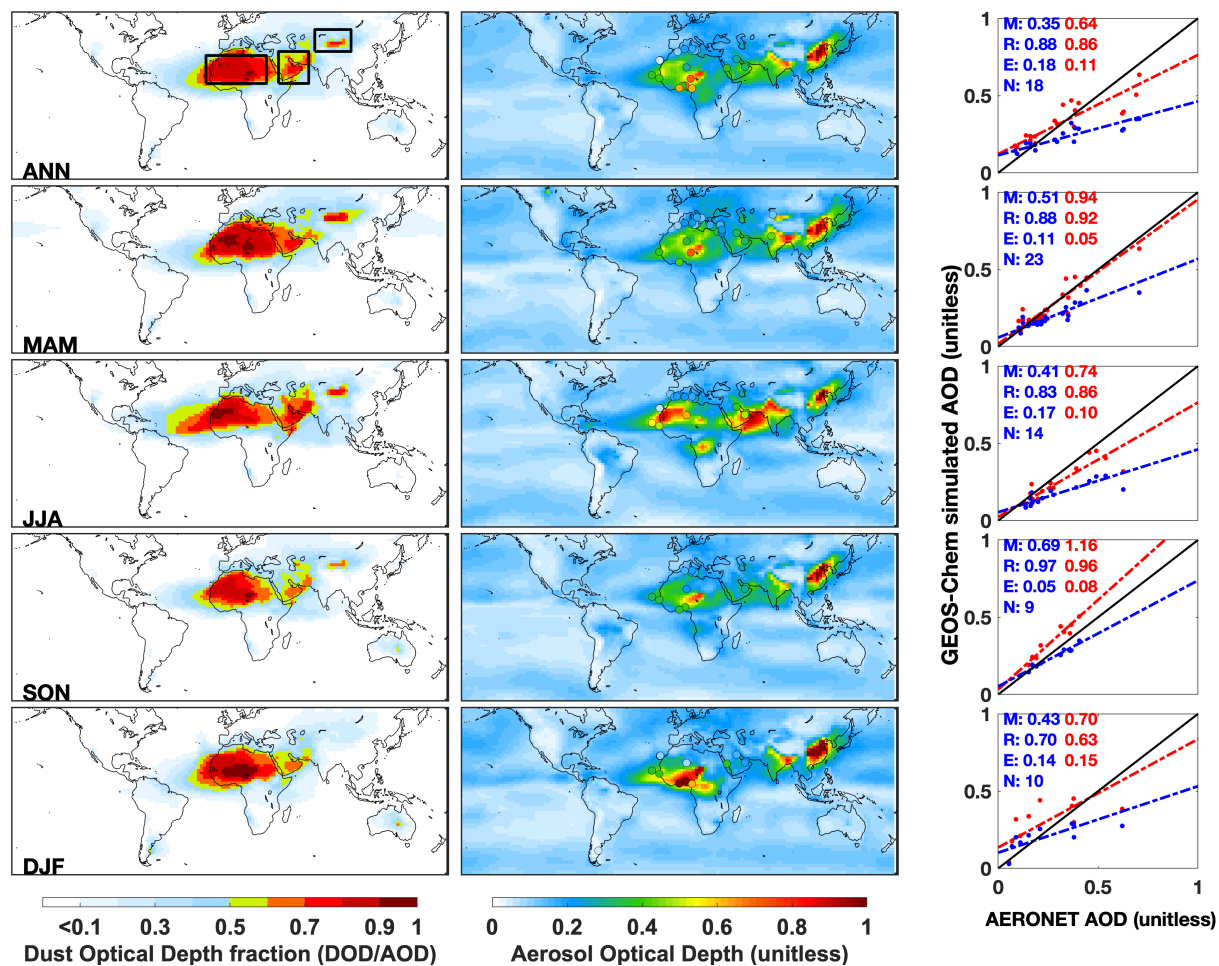
### 3.2 The performance of AOD simulations over desert regions

Figure 3 shows simulated AOD using the ~~original online and~~ updated offline dust emissions.

245 Difference maps of simulated AOD between online and offline dust emissions are shown in

Figure S7. We select for evaluation the AERONET sites where the ratio of simulated dust optical depth (DOD) to simulated total AOD exceeds 0.5 in the simulation using the updated offline dust emissions with annual dust strength of 2,000 Tg. Annually, the simulated DOD has the highest value over the Bodélé Depression. This feature persists in all seasons except summer  
250 when DOD has the highest values over the western Sahara and eastern Arabian Peninsula. The scatter plots show that annually the simulated AOD from both simulations are highly correlated with AERONET measurements across the dust regions ( $R = 0.86-0.88$ ). The simulation with updated offline dust emissions has an improved slope and smaller root mean square error than the simulation using the original online dust emissions. AOD from the simulation with updated  
255 offline dust emissions is also more consistent with the measurements in different seasons, especially in the spring (MAM) and fall (SON) with slopes close to unity and  $R$  exceeding 0.9.





260 Figure 33. Annual and seasonal mean simulated dust optical depth (DOD) fraction (left column) and  
 265 aerosol optical depth (AOD) (middle column) from GEOS-Chem simulations for 2016, and AERONET  
 measured AOD at sites where the ratio of simulated DOD and AOD exceeds 0.5, which are shown as  
 filled circles in the middle column. Boxes in the left top panel outline the three major deserts examined  
 in Figure 4. The right column shows the corresponding scatter plot with root mean square error (E),  
 correlation coefficient(R) and slope (M) calculated with reduced major axis linear regression. N is the  
 number of valid ground-based monitoring records. The results for the simulation using the original dust  
 emissions are shown in blue; the results for the simulation using updated dust emissions  
 with dust strength of  $2,000 \text{ Tg yr}^{-1}$  are shown in red. The best fit lines are dashed. The 1:1 line is solid.

270 We further evaluate the performance of simulated AOD over major desert regions using  
 the MODIS Deep Blue (DB) and MAIAC AOD products. Figure 4 shows annual and seasonal  
 scatter plots comparing GEOS-Chem simulated AOD using original online dust emissions and  
 updated offline dust emissions against retrieved AOD from MODIS DB and MAIAC satellite

products over the three major desert regions outlined in Fig. 3. Figure S86 shows the annual and seasonal AOD distribution from MODIS DB and MAIAC. Annually, the simulation using updated offline dust emissions exhibits greater consistency with satellite AOD than does the simulation using original online dust emissions across all three desert regions. The simulation using updated offline dust emission performs better across all three desert regions and in all four seasons except for the Sahara in summer, during which AOD is overestimated. Both simulations underestimate AOD over central Asian deserts during winter when dust emissions are low and other sources may be more important. Overall, the simulation using original online dust emissions underestimates AOD over all three major desert regions, especially over the Middle East and central Asian deserts. The simulation using updated offline dust emissions exhibits greater consistency with satellite observations with higher slopes and correlations.

285

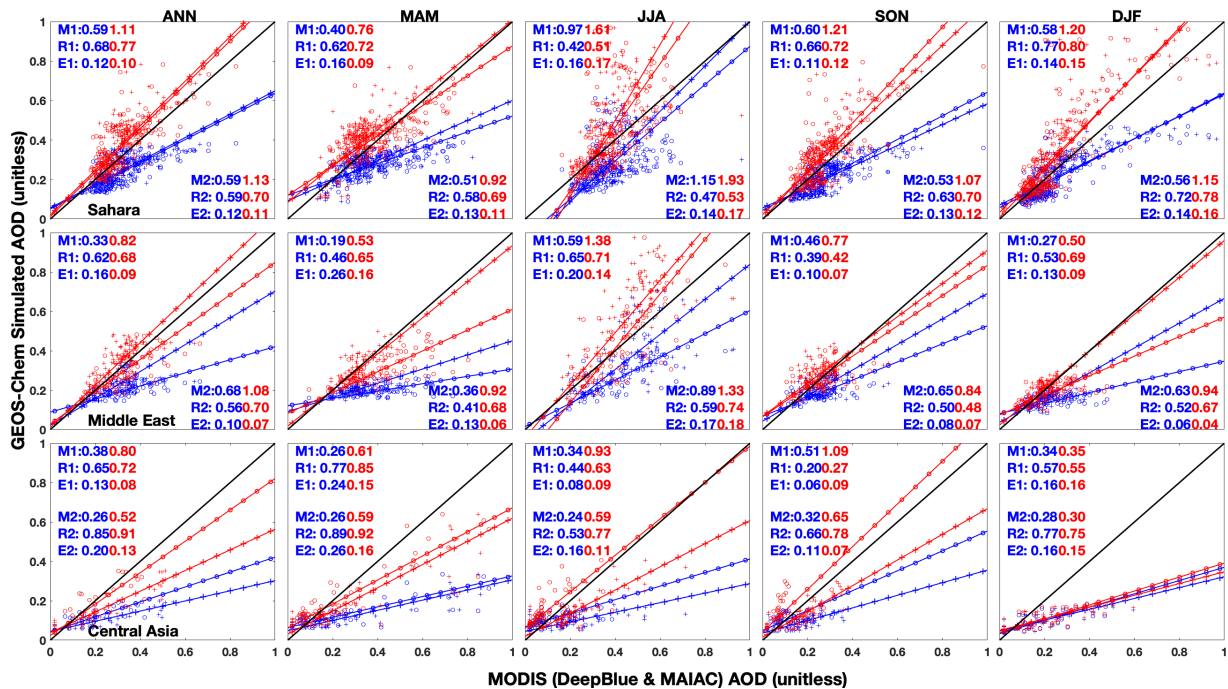
### **3.3 Evaluation of the simulations against surface dust concentration measurements**

We also evaluate our simulations using different dust emissions against measurements of surface dust concentrations. Figure 5 shows the comparison of modeled fine dust surface concentration against the fine dust concentration observation from the IMPROVE network. The simulations using the updated offline dust emissions can better represent the observed surface fine dust concentration measurements than the simulation using the original online dust emissions with higher correlations and slopes across all seasons. Annually, the correlation between the simulation and observation increases from 0.39 to 0.68 , and the slope increases from 0.31 to 0.71 when using the updated offline dust emissions with annual dust strength of 909 Tg compared to the simulation using the original online dust emissions. Scaling the annual

295

dust strength to 2,000 Tg/yr marginally improves the performance of the model simulation of fine dust concentrations in all seasons except winter, during which the surface fine dust concentrations are overestimated. Given the specificity and density of the dust measurements, and the disconnect of North American dust emissions from the global source, we conduct an additional sensitivity simulation with North American dust emissions reduced by 30%. The right column shows that the annual slope in the resultant simulation versus observations improves to 1.07, minor improvements to annual and seasonal correlations. Future efforts should focus on better representing the seasonal variation of dust emissions.

Figure 6 shows the comparison of seasonal averaged modeled and measured surface dust concentrations from 12 independent sites across the globe. The simulation using the updated offline dust emissions with dust strength of 2,000 Tg yr<sup>1</sup> is more consistent with the observations at almost all sites. The remaining bias at sites distant from source regions, for example sites in the Southern Hemisphere and East Asia, likely reflects remaining uncertainty in representing dust deposition. Further research is needed to address remaining knowledge gaps, such as better representing the dust size distribution and deposition during transport.

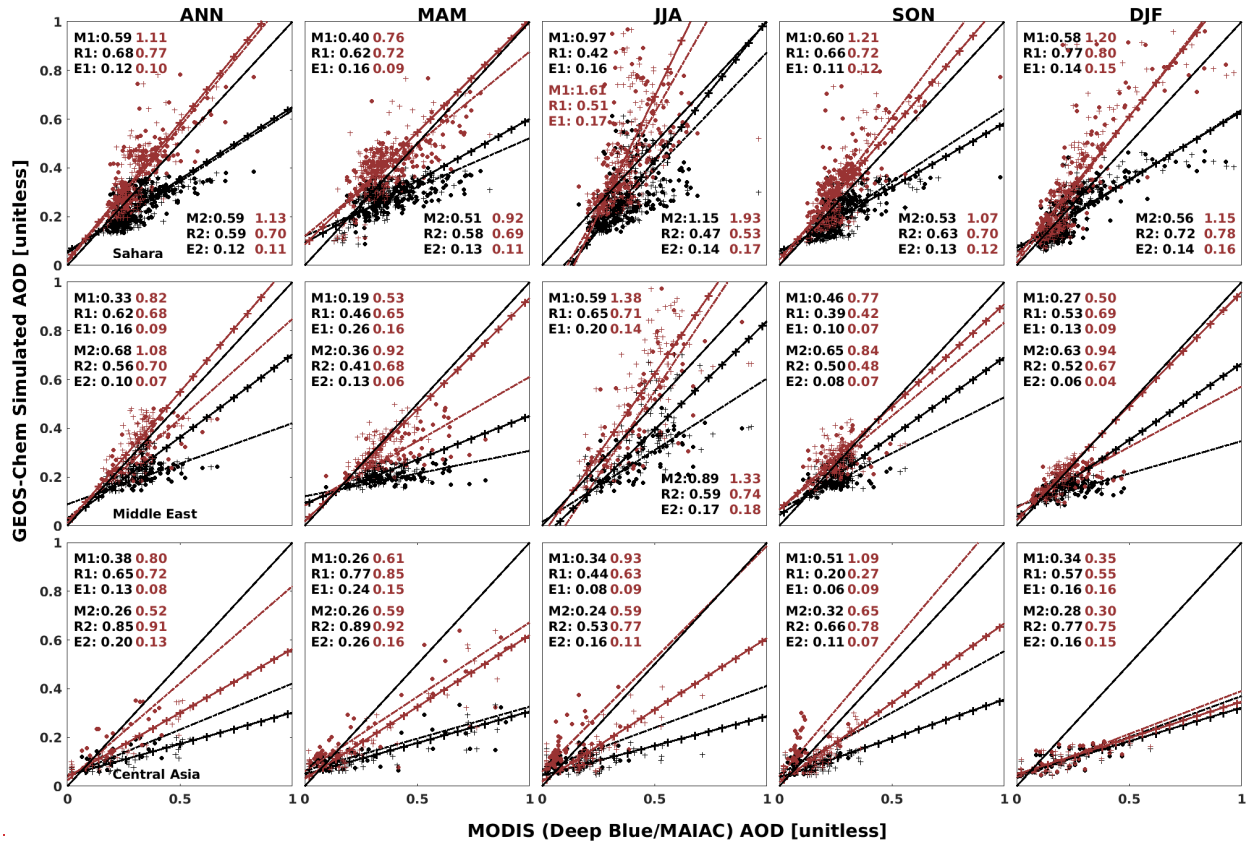


### 3.3 Discussion of the dust source strength

315 One of the advantages of the offline dust emissions is that the dust source strengths are scalable. We have found that the simulation with global total annual dust emission scaled to 2,000 Tg better represents observations than does the default simulation with global total annual dust emission of 909 Tg. We also evaluate simulations with global total annual dust emission scaled to 1,500 Tg and 2,500 Tg. Figure S7 indicates that the simulation with global total annual dust emission scaled to 2,000 Tg is more consistent with satellite observations over the Sahara and Middle East. Although the central Asian deserts and regions with AERONET observations (Fig. S8) are better represented by the simulation with global total annual dust emission scaled to 2,500 Tg, since the Sahara has the highest dust emissions (Huneeus et al., 2011), and AOD over the Sahara is most likely dominated by dust, we scale global total annual dust emissions to best match this source region. Additional development and evaluation should be conducted to further narrow the uncertainty of dust emissions, especially at the regional scale.

320

325



330

335

Figure 4. Scatter plots and statistics of comparing GEOS-Chem simulated AOD with satellite AOD over desert regions annually (the first column) and seasonally (the right four columns). The results for Sahara, Middle East and Central Asia deserts are shown in the top, middle and bottom rows respectively. The results for the simulation using the original dust emissions are shown in black; the results for the simulation using updated dust emissions with dust strength of 2,000 Tg yr<sup>-1</sup> are shown in red. Open circles ~~Dots~~ represent the comparison with MODIS Deep Blue AOD; the plus signs represent the comparison with MAIAC AOD. Correlation coefficient(R), root mean square error (E), and Slope (M) are reported, in which R1, E1 and M1 show the results of the comparison with MODIS Deep Blue AOD; R2, E2 and M2 show the results of the comparison with MAIAC AOD. The best fit lines are dashed lines with corresponding marker signs and colors. The 1:1 line solid black line.

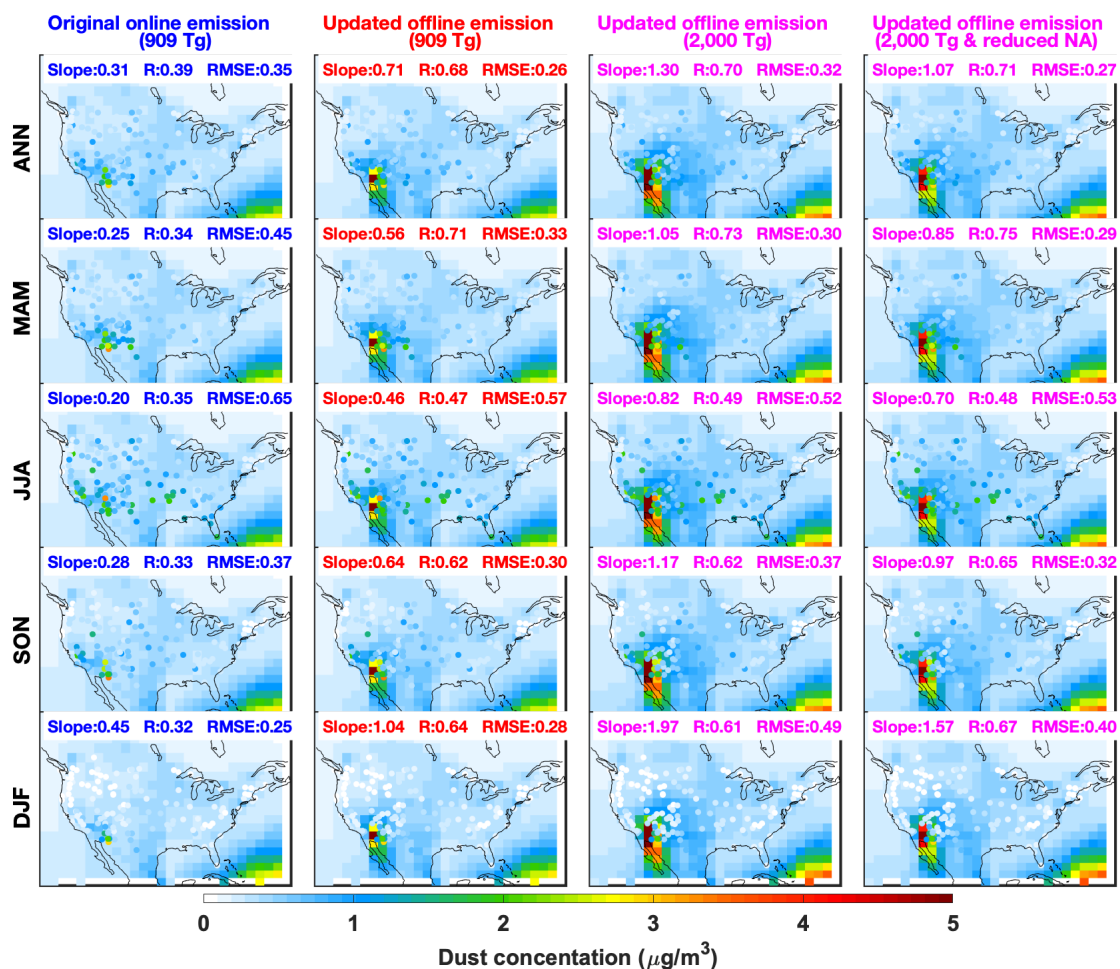
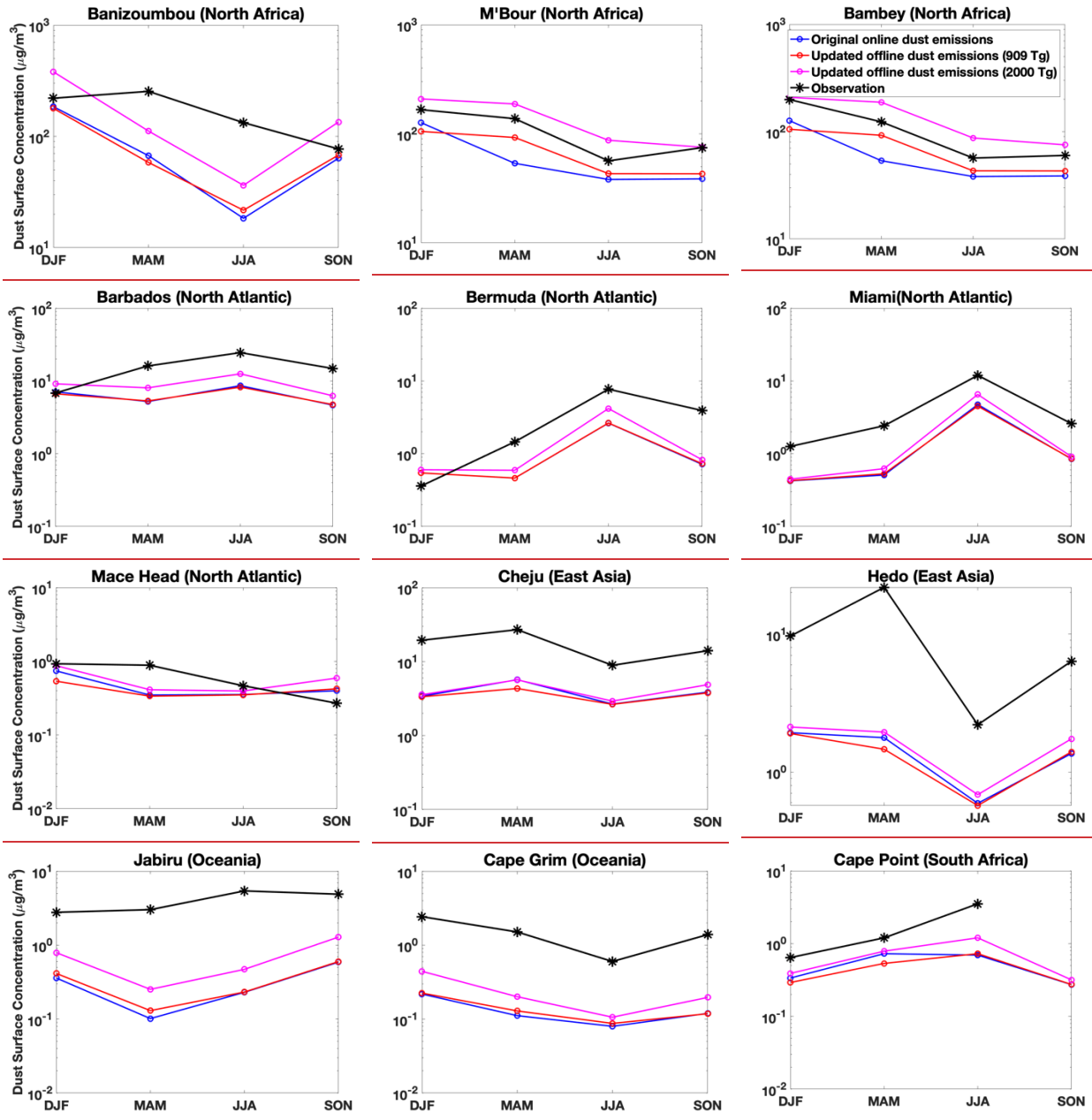


Figure 5. Annual and seasonal mean simulated fine dust concentrations from GEOS-Chem simulations with different dust emissions for 2016, and IMPROVE fine dust measurements, which are shown as filled circles. Root mean square error (E), correlation coefficient (R) and slope (M) calculated with reduced major axis linear regression are reported. The results for the simulation using the original dust emissions are shown in blue (left column); the results for the simulation using updated dust emissions with dust strength of 909 Tg yr<sup>-1</sup> are shown in red (second column); the results for the simulation using updated dust emissions with dust strength of 2,000 Tg yr<sup>-1</sup> are shown in magenta (third column); the right column is the sensitivity simulation with North America dust emission reduced by 30%.

340

345



350 Figure 6. Comparison of modeled and measured seasonal averaged surface dust concentrations at 12  
independent globally distributed sites for the years 1981-2000. Nine sites are in the dust belt across  
Northern hemisphere. The remaining 3 sites are relatively close to the weak dust emission regions in  
Southern Hemisphere. The results for the simulation using the original dust emissions are shown in blue;  
the results for the simulation using updated dust emissions with dust strength of 909 Tg yr<sup>-1</sup> are shown  
in red; the results for the simulation using updated dust emissions with dust strength of 2,000 Tg yr<sup>-1</sup> are  
shown in magenta. The measurements are in black.  
 355

### 3.4 Discussion of the dust source strength

360 One of the advantages of the offline dust emissions is that the same dust source strength can  
be readily applied to all model resolutions, facilitating evaluation of dust source strength  
independent of resolutions. We have found that the simulation with global total annual dust  
emission scaled to 2,000 Tg better represents observations than does the default simulation  
with global total annual dust emissions of 909 Tg. We also evaluate simulations with global total  
365 annual dust emission scaled to 1,500 Tg and 2,500 Tg. Figure S9 indicates that the simulation  
with global total annual dust emission scaled to 2,000 Tg is more consistent with satellite  
observations over the Sahara and Middle East. Although the central Asian deserts and regions  
with AERONET observations (Fig. S10) are better represented by the simulation with global total  
annual dust emission scaled to 2,500 Tg, since the Sahara has the highest dust emissions  
370 (Huneeus et al., 2011), and AOD over the Sahara is most likely dominated by dust, we scale  
global total annual dust emissions to best match this source region. Additional development  
and evaluation should be conducted to further narrow the uncertainty of dust emissions,  
especially at the regional scale.

#### **3.54 Advantages of high resolution offline dust emissions for model development**

375  
Uncertainty remains in the estimated global annual total dust emissions. Direct dust emission  
flux observations are few. Current atmospheric ~~and chemical transport~~ models apply a global  
scale factor to optimize with a specific set of ground observations. Because of the non-linear  
380 dependence on resolution of the dust emissions, the source strength has historically depended

upon model resolution, which inhibits general evaluation. The native resolution offline dust emissions facilitate consistent evaluation and application across all model resolutions. Such consistency is particularly important for stretched-grid simulations with the capability for factors of over 100 variation in resolution within a single simulation (Bindle et al., 2020).

385

#### 4 Summary and Conclusions

The nonlinear dependence of dust emission parameterizations upon model resolution poses a challenge for the next generation of chemical transport models with nimble capability for multiple resolutions. ~~In this paper we have developed and tested a~~The method explored here

390

to calculate offline dust emissions at ~~the~~ native meteorological resolution ~~to~~ promote consistency of dust emissions across different model resolutions. We take advantage of the capability of HEMCO standalone module to calculate dust emission offline at native

meteorological resolution using the DEAD dust emission scheme combined with an updated high resolution dust source function. We evaluate the performance of the simulation with

395

native resolution offline dust emissions and an updated dust source function with source strength of 2,000 Tg yr<sup>-1</sup>. We find better agreement with measurements, including satellite and

AERONET AOD, and surface dust concentrations. The offline fine resolution dust emissions

strengthen the dust emissions over smaller ~~better resolve smaller~~ desert regions. The

independence of source strength from simulation resolution facilitates evaluation with

400

observations. Sensitivity simulations with an annual global source strength of either 1,500 or 2,500 Tg generally degraded the performance. A sensitivity simulation with North American

emissions reduced by 30% improved the annual mean slope versus observations. ~~Future~~ ~~urther~~

work should continue to develop and evaluate the representation of dust deposition and regional seasonal variationemissions.

## 405 **5 Code and Data Availability**

The source code for generating the offline dust emissions is available on GitHub

(<https://github.com/Jun-Meng/geos-chem/tree/v11-01-Patches-UniCF-vegetation>) and Zenodo repository ( <https://doi.org/10.5281/zenodo.4062003> ) (Meng et al., 2020b). The instruction of how to generate the emission files is in the README.md file in the GitHub repository

410 (<https://github.com/Jun-Meng/geos-chem/tree/v11-01-Patches-UniCF-vegetation>). The global high resolution (0.25°x0.3125°) dust emission inventory is available on Zenodo

(<https://doi.org/10.5281/zenodo.4060248>) (Meng et al., 2020a), containing netCDF format files of global gridded hourly mineral dust emission flux rate. Currently, the dataset (version1.0) is available for the year 2016. The dataset for other years since 2014 will be available in future

415 versions.

The base GEOS-Chem source code in version 12.5.0 is available on Github

(<https://github.com/geoschem/geos-chem/tree/12.5.0>) and Zenodo repository

(<https://zenodo.org/record/3403111#.X7PKv5NKiF0,%202019>). The GEOS-Chem simulation

420 output data and AOD observations used to evaluate the model performance, including MODIS

Deep Blue, MODIS MAIAC and AERONET AOD, can be accessed via this Zenodo repository

(<https://doi.org/10.5281/zenodo.4312944>) (Meng et al., 2020c).

## **Information about the Supplement**

425 The supplement related to this article describes the details of the dust emission scheme used in  
this project, [the updated high resolution dust source function](#), as well as additional figures  
described in the main text.

### **Author contributions**

430 RVM and JM conceived the project. JM developed the dust emission dataset using data and  
algorithms from DAR, PG, MH, AvD, and MPS. JM prepared the manuscript with contributions  
from all coauthors. All authors helped revise the manuscript.

### **Competing interests**

435 The authors declare that they have no conflict of interest.

### **Acknowledgement**

This work was supported by the Natural Science and Engineering Research Council of Canada.  
Jun Meng was partially supported by a Nova Scotia Research and Innovation Graduate  
440 Scholarship. Martin acknowledges partial support from NASA AIST-18-0011. We are grateful to  
Compute Canada and Research Infrastructure Services in Washington University in St. Louis for  
computing resources. The meteorological data (GEOS-FP) used in this study have been provided  
by the Global Modeling and Assimilation Office (GMAO) at NASA Goddard Space Flight Center.  
445 [We thank Jasper Kok and Longlei Li for providing the compilation of independent surface dust  
concentrations measurements. We thank the four anonymous reviewers for their constructive  
comments and suggestions.](#) All figures are produced with the MATLAB ~~2019a~~-software.

## References

~~Graham CC Doc: <https://docs.computecanada.ca/wiki/Graham>, last access: 6~~

450 ~~March 2021.~~

Bergin, M. H., Ghoroi, C., Dixit, D., Schauer, J. J., and Shindell, D. T.: Large Reductions in Solar Energy Production Due to Dust and Particulate Air Pollution, *Environ. Sci. Technol. Lett.*, 4, 339–344, <https://doi.org/10.1021/acs.estlett.7b00197>, 2017.

455 Bindle, L., Martin, R. V., Cooper, M. J., Lundgren, E. W., Eastham, S. D., Auer, B. M., Clune, T. L., Weng, H., Lin, J., Murray, L. T., Meng, J., Keller, C. A., Pawson, S., and Jacob, D. J.: Grid-Stretching Capability for the GEOS-Chem 13.0.0 Atmospheric Chemistry Model, 1–21, <https://doi.org/10.5194/gmd-2020-398>, 2020.

Bristow, C. S., Hudson-Edwards, K. A., and Chappell, A.: Fertilizing the Amazon and equatorial Atlantic with West African dust, 37, <https://doi.org/10.1029/2010GL043486>, 2010.

460 Chen, H., Navea, J. G., Young, M. A., and Grassian, V. H.: Heterogeneous Photochemistry of Trace Atmospheric Gases with Components of Mineral Dust Aerosol, *J. Phys. Chem. A*, 115, 490–499, <https://doi.org/10.1021/jp110164j>, 2011.

465 De Longueville, F., Hountondji, Y.-C., Henry, S., and Ozer, P.: What do we know about effects of desert dust on air quality and human health in West Africa compared to other regions?, *Sci. Total Environ.*, 409, 1–8, <https://doi.org/10.1016/j.scitotenv.2010.09.025>, 2010.

470 Drury, E., Jacob, D. J., Spurr, R. J. D., Wang, J., Shinozuka, Y., Anderson, B. E., Clarke, A. D., Dibb, J., McNaughton, C., and Weber, R.: Synthesis of satellite (MODIS), aircraft (ICARTT), and surface (IMPROVE, EPA-AQS, AERONET) aerosol observations over eastern North America to improve MODIS aerosol retrievals and constrain surface aerosol concentrations and sources, 115, <https://doi.org/10.1029/2009JD012629>, 2010.

475 Eastham, S. D., Long, M. S., Keller, C. A., Lundgren, E., Yantosca, R. M., Zhuang, J., Li, C., Lee, C. J., Yannetti, M., Auer, B. M., Clune, T. L., Kouatchou, J., Putman, W. M., Thompson, M. A., Trayanov, A. L., Molod, A. M., Martin, R. V., and Jacob, D. J.: GEOS-Chem High Performance (GCHP v11-02c): a next-generation implementation of the GEOS-Chem chemical transport model for massively parallel applications, 11, 2941–2953, <https://doi.org/10.5194/gmd-11-2941-2018>, 2018.

Fairlie, T. D., Jacob, D. J., and Park, R. J.: The impact of transpacific transport of mineral dust in the United States, *Atmospheric Environment*, 41, 1251–1266, <https://doi.org/10.1016/j.atmosenv.2006.09.048>, 2007.

- 480 Fountoukis, C. and Nenes, A.: ISORROPIA II: A computationally efficient thermodynamic equilibrium model for  $K^+$ - $Ca^{2+}$ - $Mg^{2+}$ - $NH_4^+$ - $Na^+$ - $SO_4^{2-}$ - $NO_3^-$ - $Cl^-$ - $H_2O$  aerosols, 7, 4639–4659, <https://doi.org/10.5194/acp-7-4639-2007>, 2007.
- Giles, D. M., Sinyuk, A., Sorokin, M. G., Schafer, J. S., Smirnov, A., Slutsker, I., Eck, T. F., Holben, B. N., Lewis, J. R., Campbell, J. R., Welton, E. J., Korin, S. V., and Lyapustin, A. I.: Advancements  
485 in the Aerosol Robotic Network (AERONET) Version 3 database – automated near-real-time quality control algorithm with improved cloud screening for Sun photometer aerosol optical depth (AOD) measurements, 12, 169–209, <https://doi.org/10.5194/amt-12-169-2019>, 2019.
- Gillette, D. A.: A qualitative geophysical explanation for hot spot dust emitting source regions, *Contrib. atmos. phys*, 72, 67–77, 1999.
- 490 Gillette, D. A. and Passi, R.: Modeling dust emission caused by wind erosion, 93, 14233–14242, <https://doi.org/10.1029/JD093iD11p14233>, 1988.
- Ginoux, P., Chin, M., Tegen, I., Prospero, J. M., Holben, B., Dubovik, O., and Lin, S.-J.: Sources and distributions of dust aerosols simulated with the GOCART model, 106, 20255–20273, <https://doi.org/10.1029/2000JD000053>, 2001.
- 495 Ginoux, P., Prospero, J. M., Gill, T. E., Hsu, N. C., and Zhao, M.: Global-scale attribution of anthropogenic and natural dust sources and their emission rates based on MODIS Deep Blue aerosol products, 50, <https://doi.org/10.1029/2012RG000388>, 2012.
- Hammer, M. S., Martin, R. V., van Donkelaar, A., Burchard, V., Torres, O., Ridley, D. A., and Spurr, R. J. D.: Interpreting the ultraviolet aerosol index observed with the OMI satellite instrument to  
500 understand absorption by organic aerosols: implications for atmospheric oxidation and direct radiative effects, 16, 2507–2523, <https://doi.org/10.5194/acp-16-2507-2016>, 2016.
- Holben, B. N., Eck, T. F., Slutsker, I., Tanré, D., Buis, J. P., Setzer, A., Vermote, E., Reagan, J. A., Kaufman, Y. J., Nakajima, T., Lavenu, F., Jankowiak, I., and Smirnov, A.: AERONET—A Federated Instrument Network and Data Archive for Aerosol Characterization, Remote Sensing of  
505 Environment, 66, 1–16, [https://doi.org/10.1016/S0034-4257\(98\)00031-5](https://doi.org/10.1016/S0034-4257(98)00031-5), 1998.
- Hsu, N. C., Jeong, M.-J., Bettenhausen, C., Sayer, A. M., Hansell, R., Seftor, C. S., Huang, J., and Tsay, S.-C.: Enhanced Deep Blue aerosol retrieval algorithm: The second generation, 118, 9296–9315, <https://doi.org/10.1002/jgrd.50712>, 2013.
- Huneus, N., Schulz, M., Balkanski, Y., Griesfeller, J., Prospero, J., Kinne, S., Bauer, S., Boucher, O., Chin, M., Dentener, F., Diehl, T., Easter, R., Fillmore, D., Ghan, S., Ginoux, P., Grini, A.,  
510 Horowitz, L., Koch, D., Krol, M. C., Landing, W., Liu, X., Mahowald, N., Miller, R., Morcrette, J.-J., Myhre, G., Penner, J., Perlwitz, J., Stier, P., Takemura, T., and Zender, C. S.: Global dust model intercomparison in AeroCom phase I, 11, 7781–7816, <https://doi.org/10.5194/acp-11-7781-2011>, 2011.

- 515 Jaeglé, L., Quinn, P. K., Bates, T. S., Alexander, B., and Lin, J.-T.: Global distribution of sea salt aerosols: new constraints from in situ and remote sensing observations, 11, 3137–3157, <https://doi.org/10.5194/acp-11-3137-2011>, 2011.
- Keller, C. A., Long, M. S., Yantosca, R. M., Da Silva, A. M., Pawson, S., and Jacob, D. J.: HEMCO v1.0: a versatile, ESMF-compliant component for calculating emissions in atmospheric models, 520 7, 1409–1417, <https://doi.org/10.5194/gmd-7-1409-2014>, 2014.
- Kok, J. F., Adebisi, A. A., Albani, S., Balkanski, Y., Checa-Garcia, R., Chin, M., Colarco, P. R., Hamilton, D. S., Huang, Y., Ito, A., Klose, M., Leung, D. M., Li, L., Mahowald, N. M., Miller, R. L., Obiso, V., Pérez García-Pando, C., Rocha-Lima, A., Wan, J. S., and Whicker, C. A.: Improved representation of the global dust cycle using observational constraints on dust properties and 525 abundance, 1–45, <https://doi.org/10.5194/acp-2020-1131>, 2020.
- Kosmopoulos, P. G., Kazadzis, S., Taylor, M., Athanasopoulou, E., Speyer, O., Raptis, P. I., Marinou, E., Proestakis, E., Solomos, S., Gerasopoulos, E., Amiridis, V., Bais, A., and Kontoes, C.: Dust impact on surface solar irradiance assessed with model simulations, satellite observations and ground-based measurements, 10, 2435–2453, <https://doi.org/10.5194/amt-10-2435-2017>, 530 2017.
- Latimer, R. N. C. and Martin, R. V.: Interpretation of measured aerosol mass scattering efficiency over North America using a chemical transport model, 19, 2635–2653, <https://doi.org/10.5194/acp-19-2635-2019>, 2019.
- Liu, H., Jacob, D., Bey, I., and Yantosca, R.: Constraints from <sup>210</sup>Pb and <sup>7</sup>Be on wet deposition and transport in a global three-dimensional chemical tracer model driven by assimilated 535 meteorological fields, 106, <https://doi.org/10.1029/2000JD900839>, 2001.
- Lyapustin, A., Wang, Y., Korokin, S., and Huang, D.: MODIS Collection 6 MAIAC algorithm, 11, 5741–5765, <https://doi.org/10.5194/amt-11-5741-2018>, 2018.
- Marais, E. A., Jacob, D. J., Jimenez, J. L., Campuzano-Jost, P., Day, D. A., Hu, W., Krechmer, J., 540 Zhu, L., Kim, P. S., Miller, C. C., Fisher, J. A., Travis, K., Yu, K., Hanisco, T. F., Wolfe, G. M., Arkinson, H. L., Pye, H. O. T., Froyd, K. D., Liao, J., and McNeill, V. F.: Aqueous-phase mechanism for secondary organic aerosol formation from isoprene: Application to the southeast United States and co-benefit of SO<sub>2</sub> emission controls, 16, 1603–1618, <https://doi.org/10.5194/acp-16-1603-2016>, 2016.
- 545 Martin, R. V., Jacob, D. J., Yantosca, R. M., Chin, M., and Ginoux, P.: Global and regional decreases in tropospheric oxidants from photochemical effects of aerosols, 108, <https://doi.org/10.1029/2002JD002622>, 2003.
- Meng, J., Martin, R. V., Ginoux, P., Ridley, D. A., and Sulprizio, M. P.: Global High Resolution Dust Emission Inventory for Chemical Transport Models (Version 2020\_v1.0), 550 <https://doi.org/10.5281/zenodo.4060248>, 2020a.

- Meng, J., Martin, R. V., and Ridley, D. A.: Offline\_Dust\_Emissions\_SourceCode\_2020\_v1.0, <https://doi.org/10.5281/zenodo.4062003>, 2020b.
- 555 Park, R. J., Jacob, D. J., Chin, M., and Martin, R. V.: Sources of carbonaceous aerosols over the United States and implications for natural visibility, 108, 4355, <https://doi.org/10.1029/2002JD003190>, 2003.
- Park, R. J., Jacob, D. J., Field, B. D., Yantosca, R. M., and Chin, M.: Natural and transboundary pollution influences on sulfate-nitrate-ammonium aerosols in the United States: Implications for policy, 109, <https://doi.org/10.1029/2003JD004473>, 2004.
- 560 Pye, H. O. T., Chan, A. W. H., Barkley, M. P., and Seinfeld, J. H.: Global modeling of organic aerosol: The importance of reactive nitrogen (NO<sub>x</sub> and NO<sub>3</sub>), 10, 11261–11276, <https://doi.org/10.5194/acp-10-11261-2010>, 2010.
- Ridley, D. A., Heald, C. L., and Ford, B.: North African dust export and deposition: A satellite and model perspective, *Journal of Geophysical Research: Atmospheres*, 117, <https://doi.org/10.1029/2011JD016794>, 2012.
- 565 Ridley, D. A., Heald, C. L., Pierce, J. R., and Evans, M. J.: Toward resolution-independent dust emissions in global models: Impacts on the seasonal and spatial distribution of dust, 40, 2873–2877, <https://doi.org/10.1002/grl.50409>, 2013.
- 570 Ridley, D. A., Heald, C. L., Kok, J. F., and Zhao, C.: An observationally constrained estimate of global dust aerosol optical depth, 16, 15097–15117, <https://doi.org/10.5194/acp-16-15097-2016>, 2016.
- Sayer, A. M., Munchak, L. A., Hsu, N. C., Levy, R. C., Bettenhausen, C., and Jeong, M.-J.: MODIS Collection 6 aerosol products: Comparison between Aqua’s e-Deep Blue, Dark Target, and “merged” data sets, and usage recommendations, 119, 13,965-13,989, <https://doi.org/10.1002/2014JD022453>, 2014.
- 575 Schepanski, K., Tegen, I., and Macke, A.: Comparison of satellite based observations of Saharan dust source areas, *Remote Sensing of Environment*, 123, 90–97, <https://doi.org/10.1016/j.rse.2012.03.019>, 2012.
- Shao, Y., Raupach, M. R., and Findlater, P. A.: Effect of saltation bombardment on the entrainment of dust by wind, 98, 12719–12726, <https://doi.org/10.1029/93JD00396>, 1993.
- 580 Tang, M., Huang, X., Lu, K., Ge, M., Li, Y., Cheng, P., Zhu, T., Ding, A., Zhang, Y., Gligorovski, S., Song, W., Ding, X., Bi, X., and Wang, X.: Heterogeneous reactions of mineral dust aerosol: implications for tropospheric oxidation capacity, 17, 11727–11777, <https://doi.org/10.5194/acp-17-11727-2017>, 2017.
- 585 The International GEOS-Chem User Community: geoschem/geos-chem: GEOS-Chem 12.5.0 (Version 12.5.0), Zenodo, <https://doi.org/10.5281/zenodo.3403111>, 2019.

- Wang, Q., Jacob, D. J., Spackman, J. R., Perring, A. E., Schwarz, J. P., Moteki, N., Marais, E. A., Ge, C., Wang, J., and Barrett, S. R. H.: Global budget and radiative forcing of black carbon aerosol: Constraints from pole-to-pole (HIPPO) observations across the Pacific, 119, 195–206, <https://doi.org/10.1002/2013JD020824>, 2014.
- 590 Yu, H., Chin, M., Yuan, T., Bian, H., Remer, L. A., Prospero, J. M., Omar, A., Winker, D., Yang, Y., Zhang, Y., Zhang, Z., and Zhao, C.: The fertilizing role of African dust in the Amazon rainforest: A first multiyear assessment based on data from Cloud-Aerosol Lidar and Infrared Pathfinder Satellite Observations, 42, 1984–1991, <https://doi.org/10.1002/2015GL063040>, 2015.
- 595 Yu, Y., Kalashnikova, O. V., Garay, M. J., Lee, H., and Notaro, M.: Identification and Characterization of Dust Source Regions Across North Africa and the Middle East Using MISR Satellite Observations, 45, 6690–6701, <https://doi.org/10.1029/2018GL078324>, 2018.
- Zender, C. S., Bian, H., and Newman, D.: Mineral Dust Entrainment and Deposition (DEAD) model: Description and 1990s dust climatology, 108, <https://doi.org/10.1029/2002JD002775>, 2003.
- 600 Zender, C. S., Miller, R. L. R. L., and Tegen, I.: Quantifying mineral dust mass budgets: Terminology, constraints, and current estimates, 85, 509–512, <https://doi.org/10.1029/2004EO480002>, 2004.
- 605 Zhang, L., Kok, J. F., Henze, D. K., Li, Q., and Zhao, C.: Improving simulations of fine dust surface concentrations over the western United States by optimizing the particle size distribution, 40, 3270–3275, <https://doi.org/10.1002/grl.50591>, 2013.

## Supplement

### S1. Description of the Dust Emission Parameterization

The dust detrainment and deposition (DEAD) scheme (Zender et al., 2003) is based on a theory studying the transport of dust by winds ~~on Mars~~ by White (1979) to calculate horizontal dust saltation flux  $H$ :

$$H = C \frac{\rho}{g} U^{*3} \left(1 - \frac{U_t^*}{U^*}\right) \left(1 + \frac{U_t^*}{U^*}\right)^2 \quad (1)$$

where  $C$  is a global tuning factor determining the total dust strength,  $\rho$  is the air density,  $g$  is the acceleration of gravity,  $U^*$  is the friction velocity and  $U_t^*$  is the threshold friction velocity. The vertical dust flux  $F$ , is proportional to the horizontal saltation flux  $H$  is parameterized as:

$$F = A_m S \alpha H, \quad (2)$$

where  $\alpha$  is the sandblasting mass efficiency, which is a function of the clay fraction in the soil.

We use a fixed soil clay fraction of 0.2 as suggested in Zender et al. (2003).  $S$  is dust source function, which is an effective factor that favors emissions from specific geographic features.

We updated  $S$  with a fine resolution dataset without vegetation mask [as described in Sect. S2](#)

[Ginoux et al. \(2001\)](#).  $A_m$  is a factor that suppresses dust emissions from snow covered land ( $A_s$ ), wetlands ( $A_i$ ) and water bodies ( $A_w$ ) and vegetated area ( $A_v$ ),

$$A_m = (1 - A_s)(1 - A_i - A_w)(1 - A_v) \quad (3)$$

The vegetation effect  $A_v$  is represented by monthly mean leaf plus stem area index (LAI)

following Zender et al. (2003). This feature enables seasonal dust mobilization in the dust

emission scheme. We have not investigated ~~inter~~the annual vegetation variation in this study.

## **S2. Description of the Updated Source Function**

The updated source function provides erodibility factors for sparsely vegetated surfaces with a potential for accumulated fine sediments. The potential location of accumulated sediments has been determined by comparing the elevation of any 1 x 1 degree grid point with its surrounding hydrological basin using the same equation 1 of Ginoux et al. (2001). The updated source function is then linearly interpolated to a 0.25 degree Cartesian grid and multiplied by the fraction of bare surface within the grid cell. Such surfaces are obtained globally from the classes 8 (bare ground) and 9 (shrubs and bare ground) of the land cover inventory retrieved from the multi-year 8 km AVHRR data (Defries et al., 2000). It is assumed that 100% of class 8 is bare, while only 20% for class 9. According to the survey by the Chinese Academy of Sciences (CAS, 1998), desertification has increased the bare sandy lands in China. To include these barren lands, we follow the methodology followed by (Gong et al., 2003) to use the Chinese Desertification Map (Sunling Gong personal communication) and consider the desertification classes 1 (serious desertification soil), 2 (heavy desertification soil), 3 (current desertification soil) with 80% erodible bare surface, and classes 4 (potential desertification soil) and 5 (low-grade desertification soil) with 60% erodible bare surface.

~~S2. Computational time required for calculating offline dust emissions~~

## Supplemental Figures

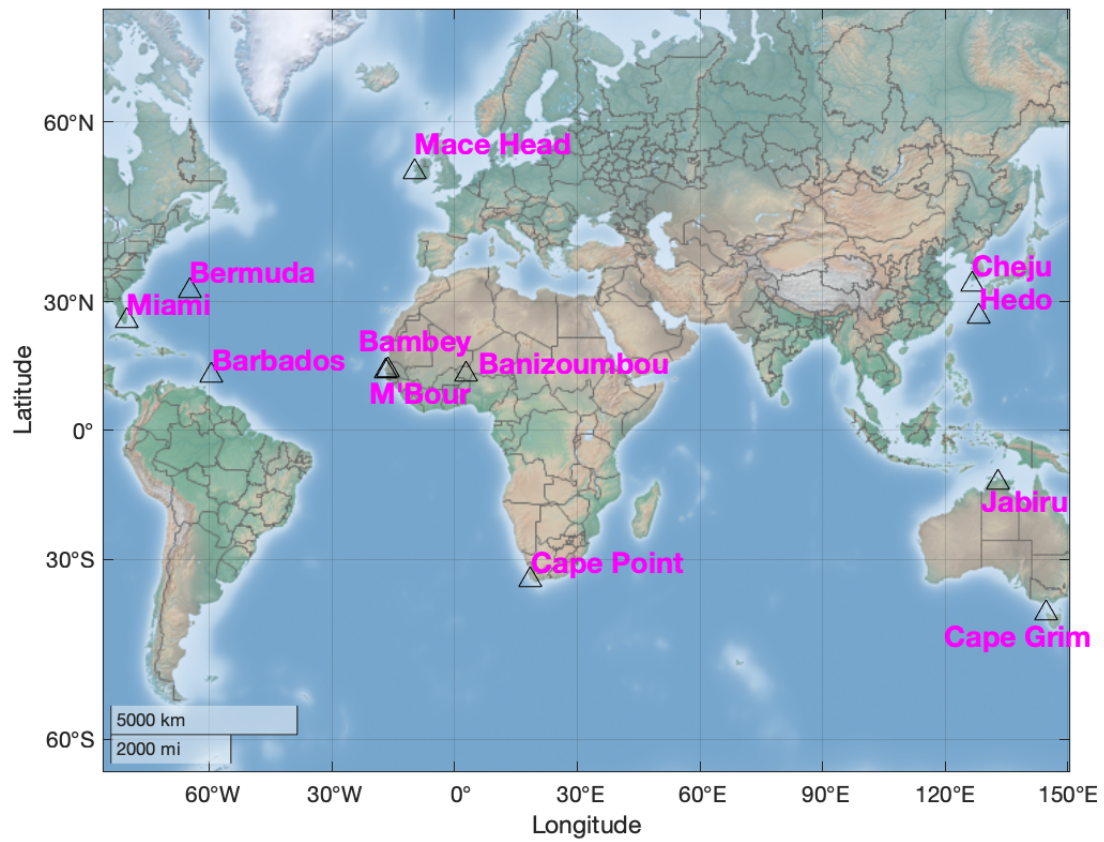


Figure S1. Geolocations of the 12 independent sites used in Figure 6 of the main text.

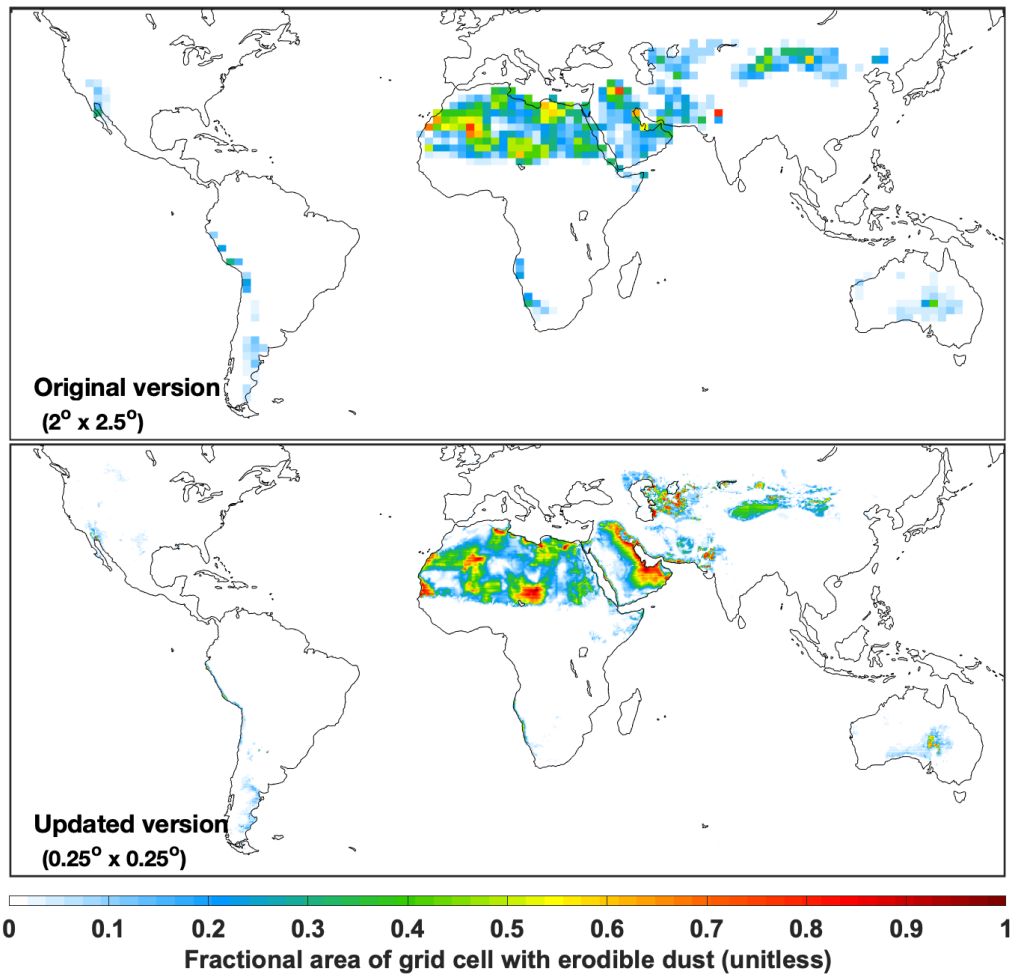


Figure S24. The original and updated versions of the dust source function.

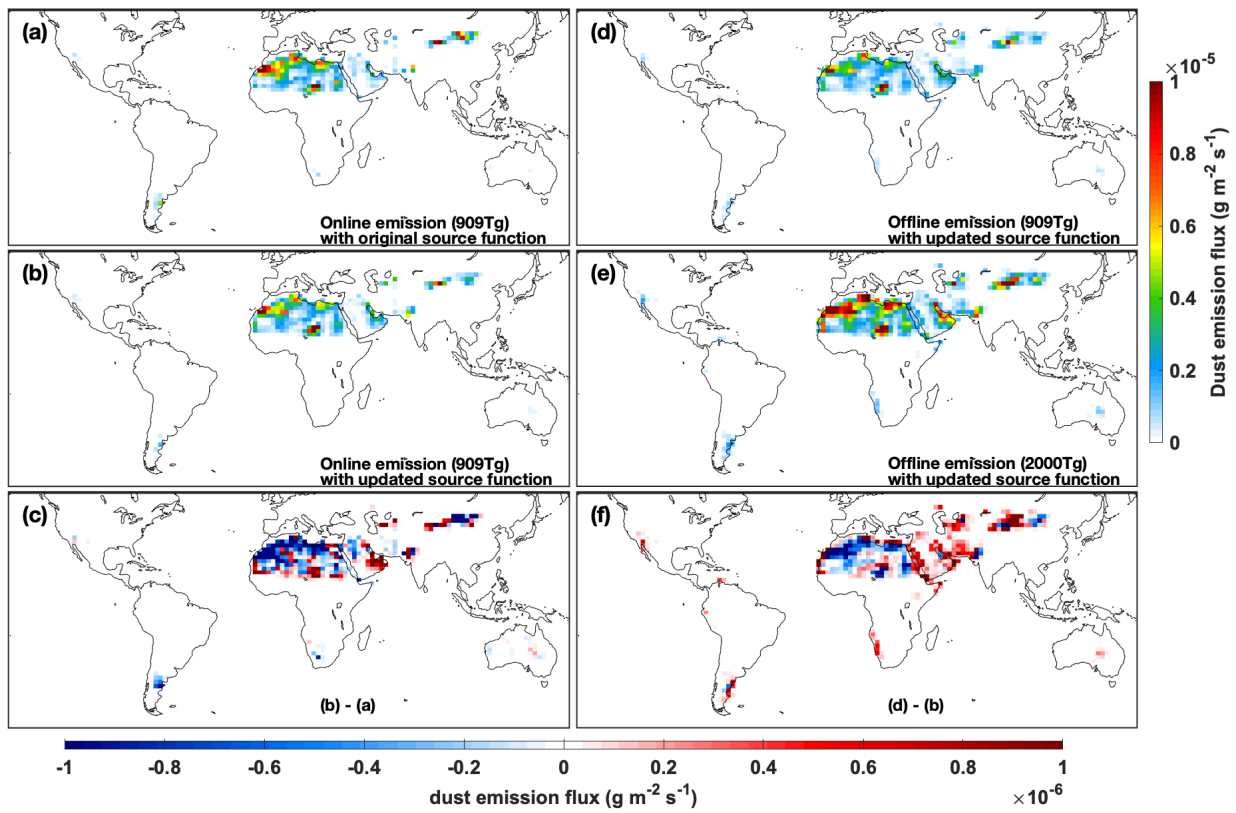
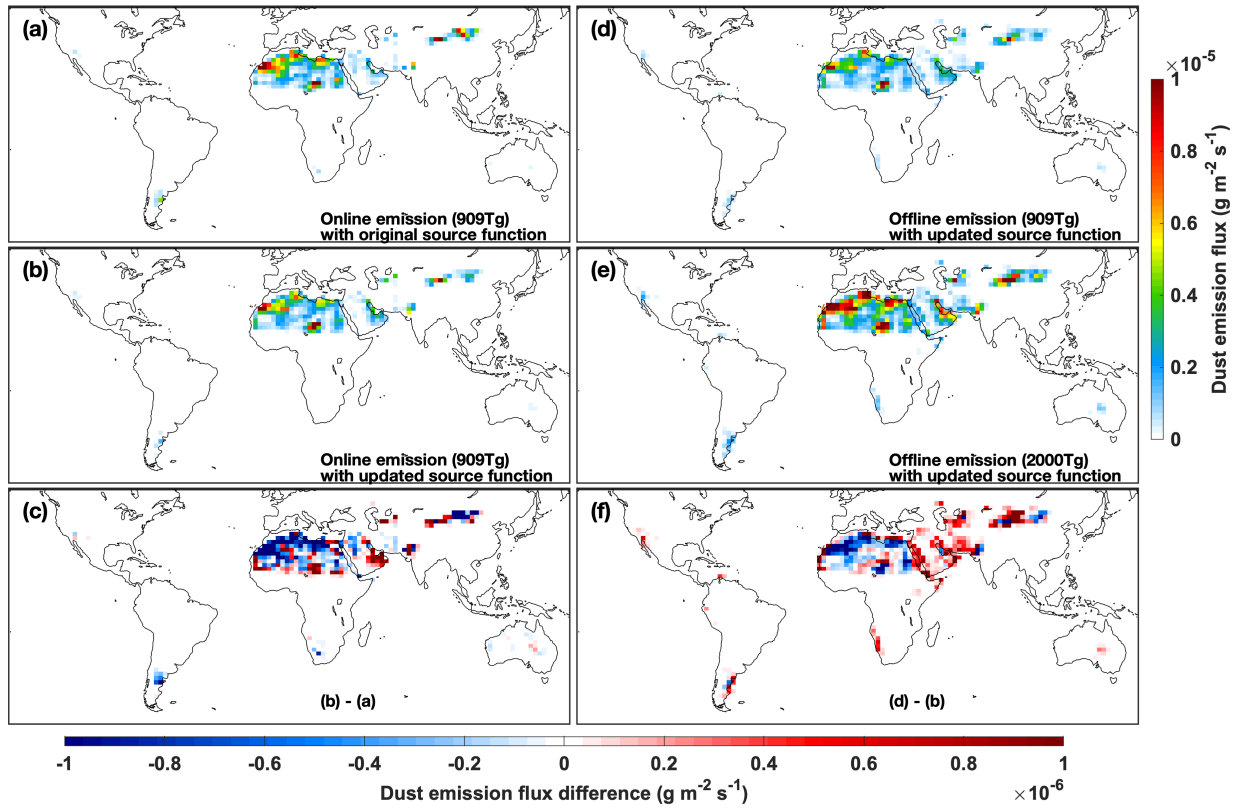
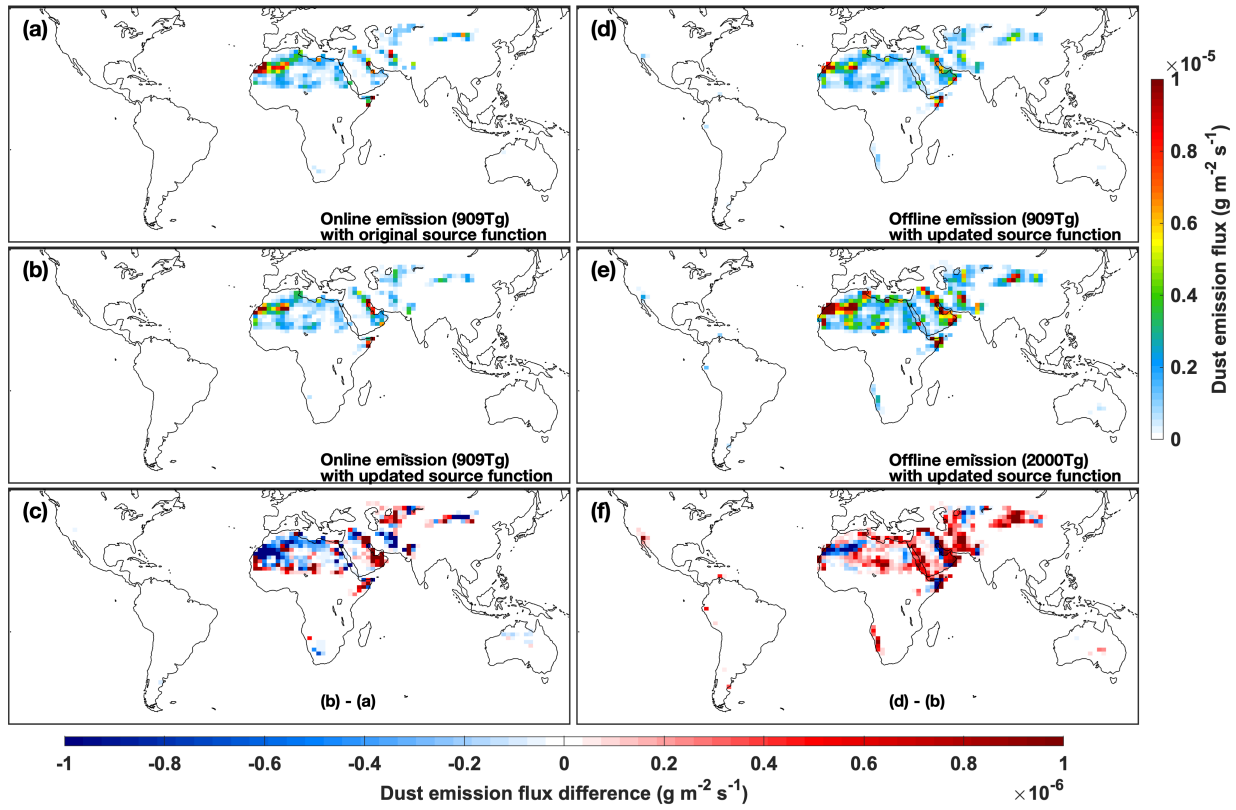


Figure S32. ~~The same as in~~ Fig. 2 but averaged over MAM (March, April and May).



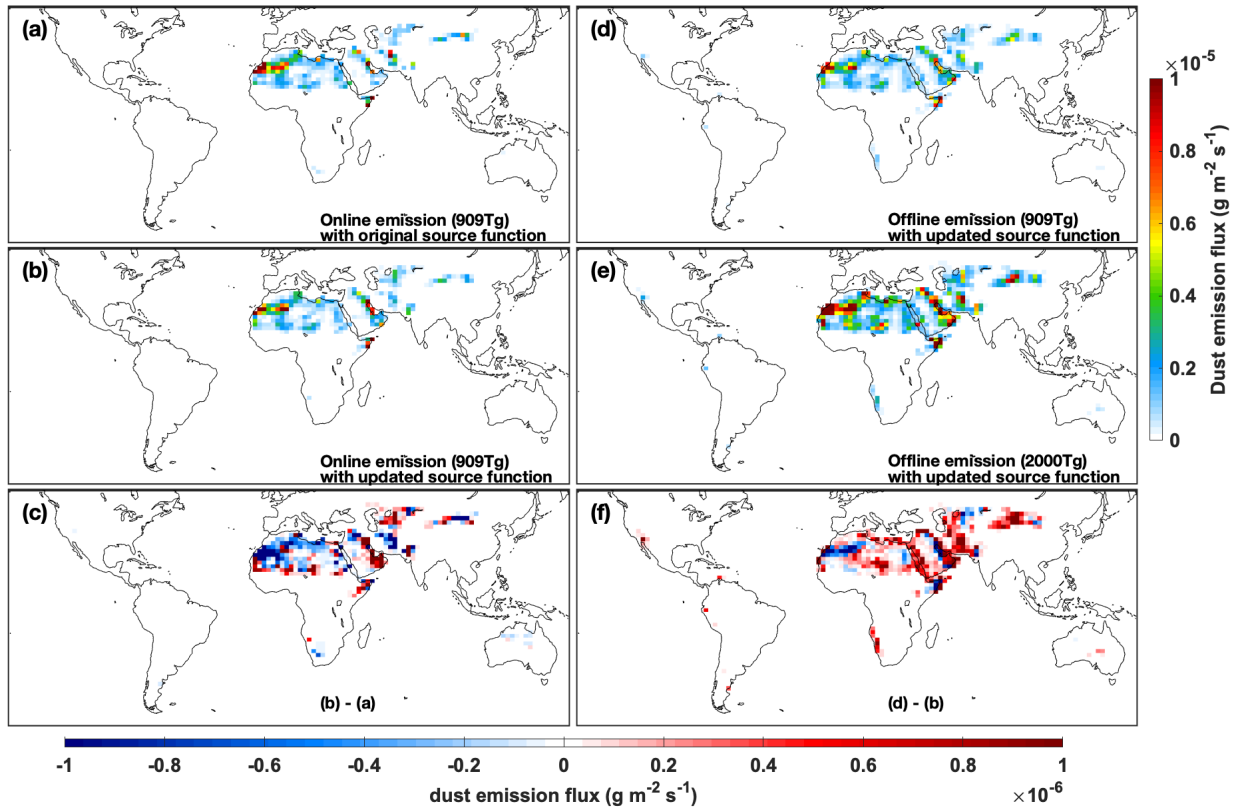
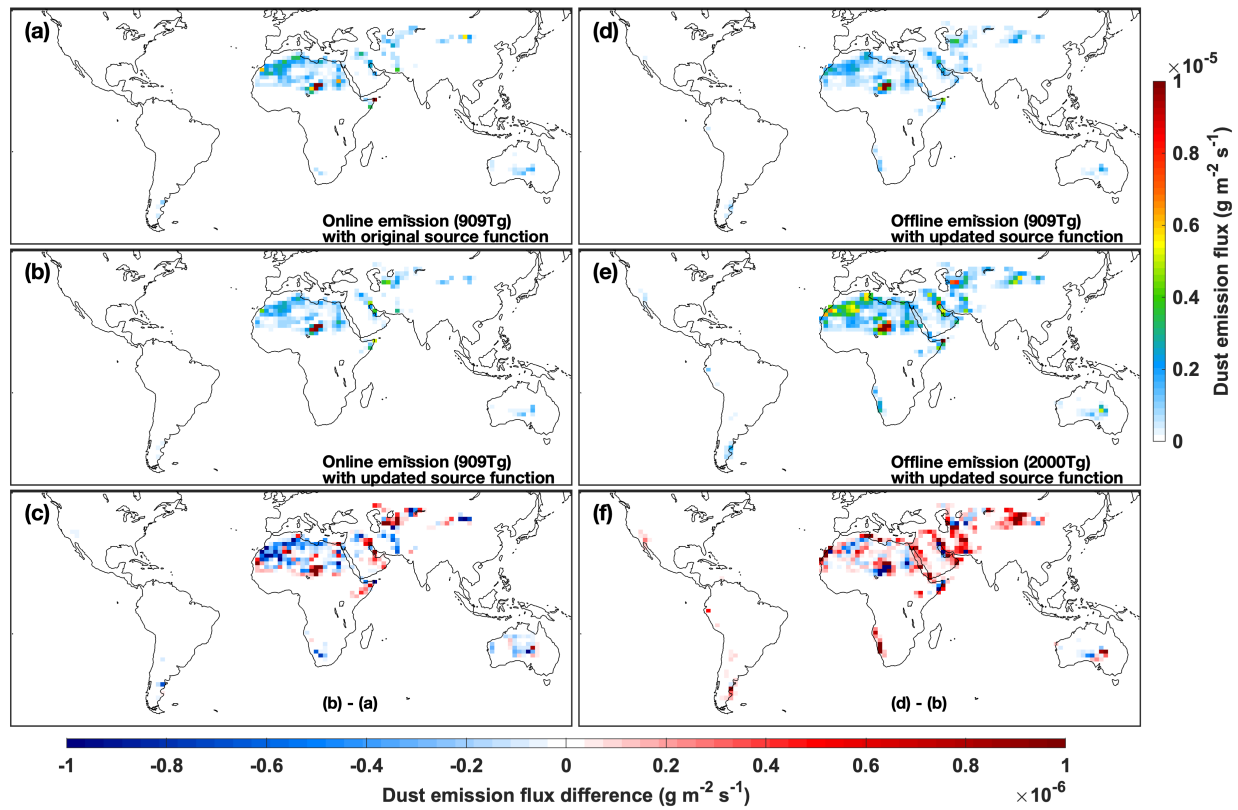


Figure S43. ~~As in~~The same as Fig. 2 but averaged over JJA (June, July and August).



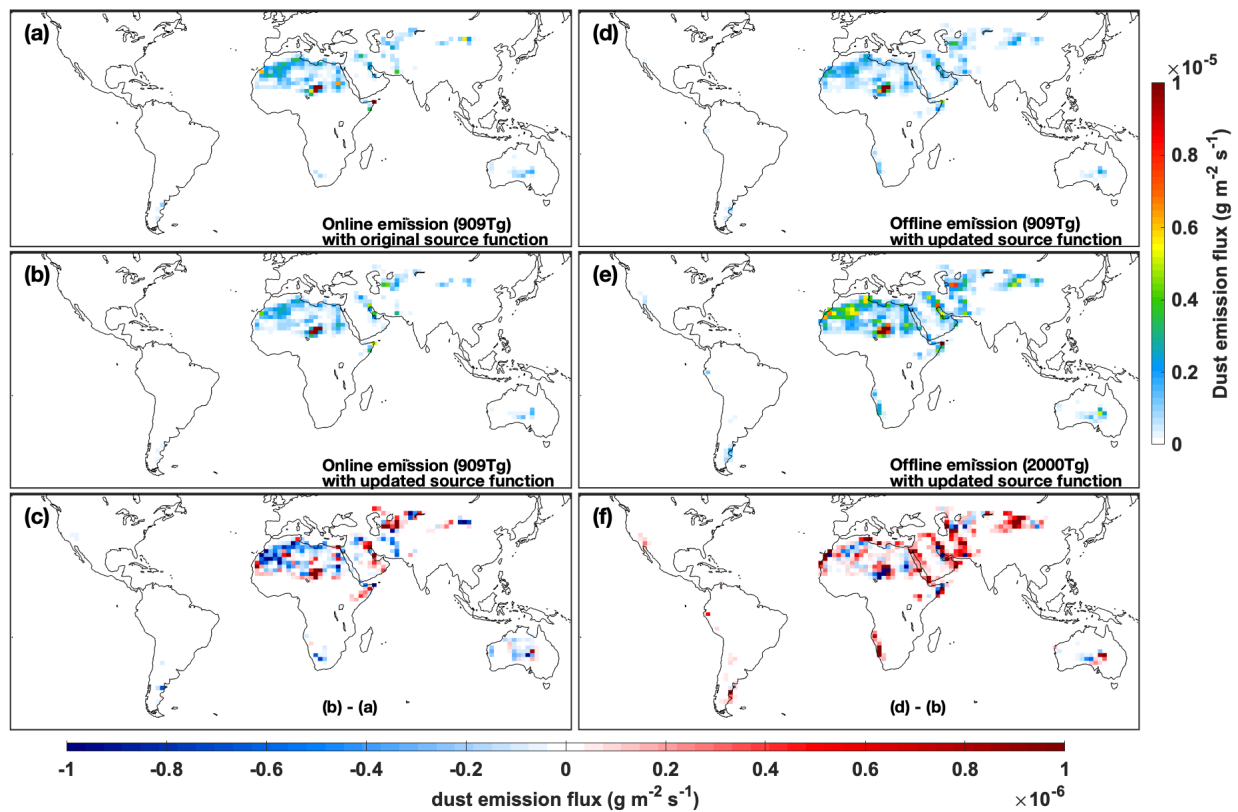
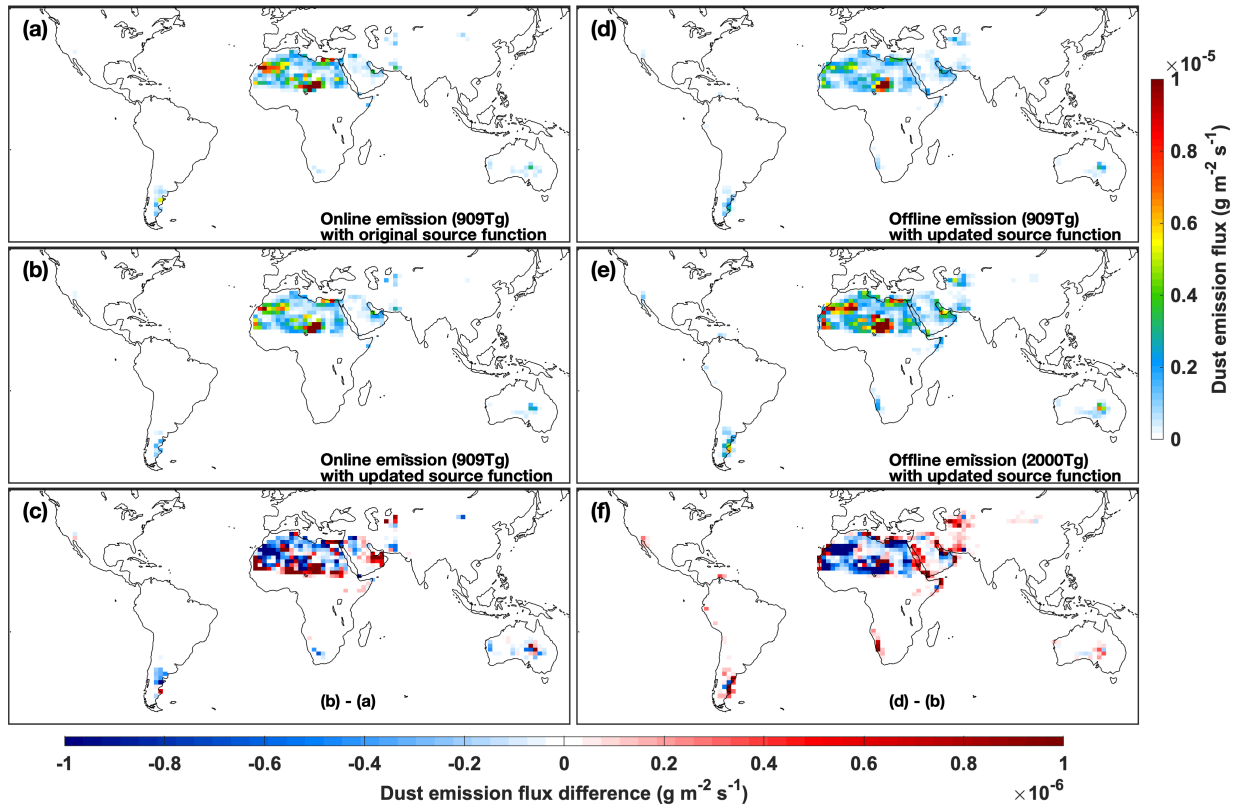


Figure S54. The same as As in Fig. 2 but averaged over SON (September, October and November).



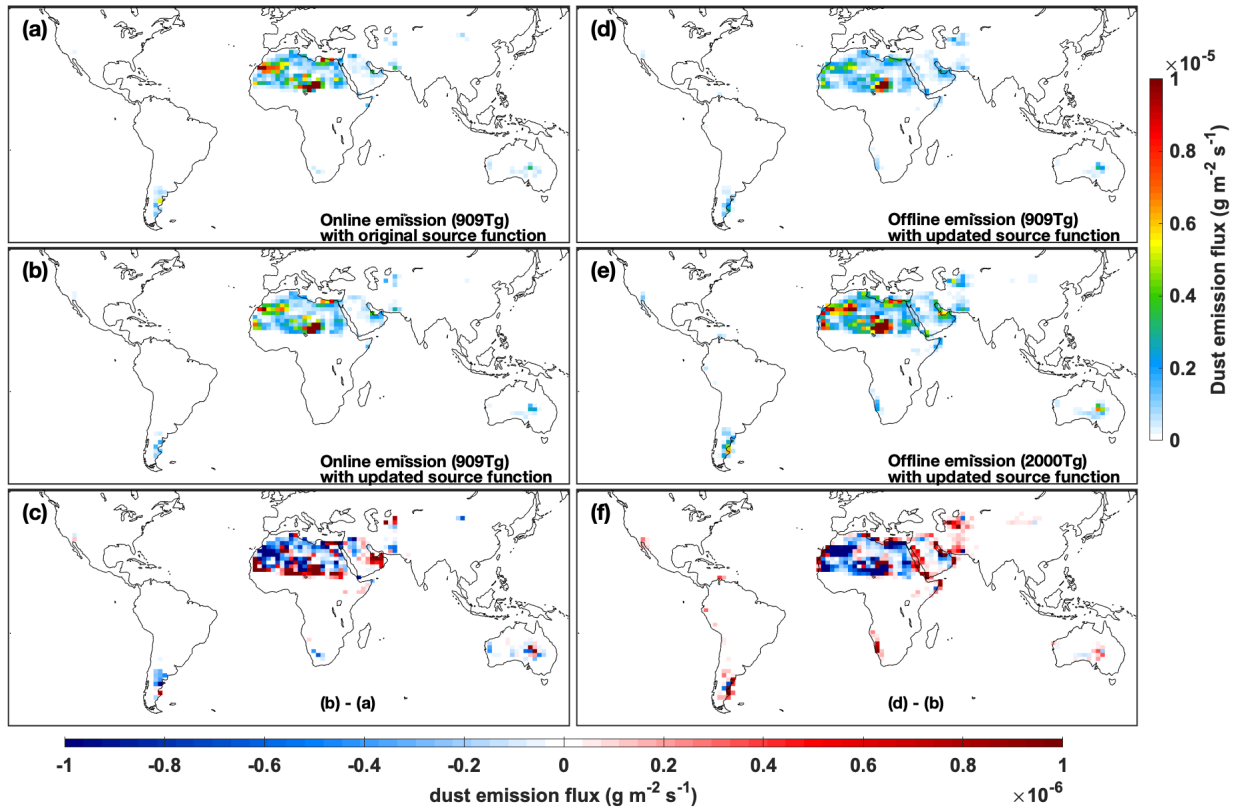


Figure S65. As in ~~The same as~~ Fig. 2 but averaged over DJF (December, January and February).

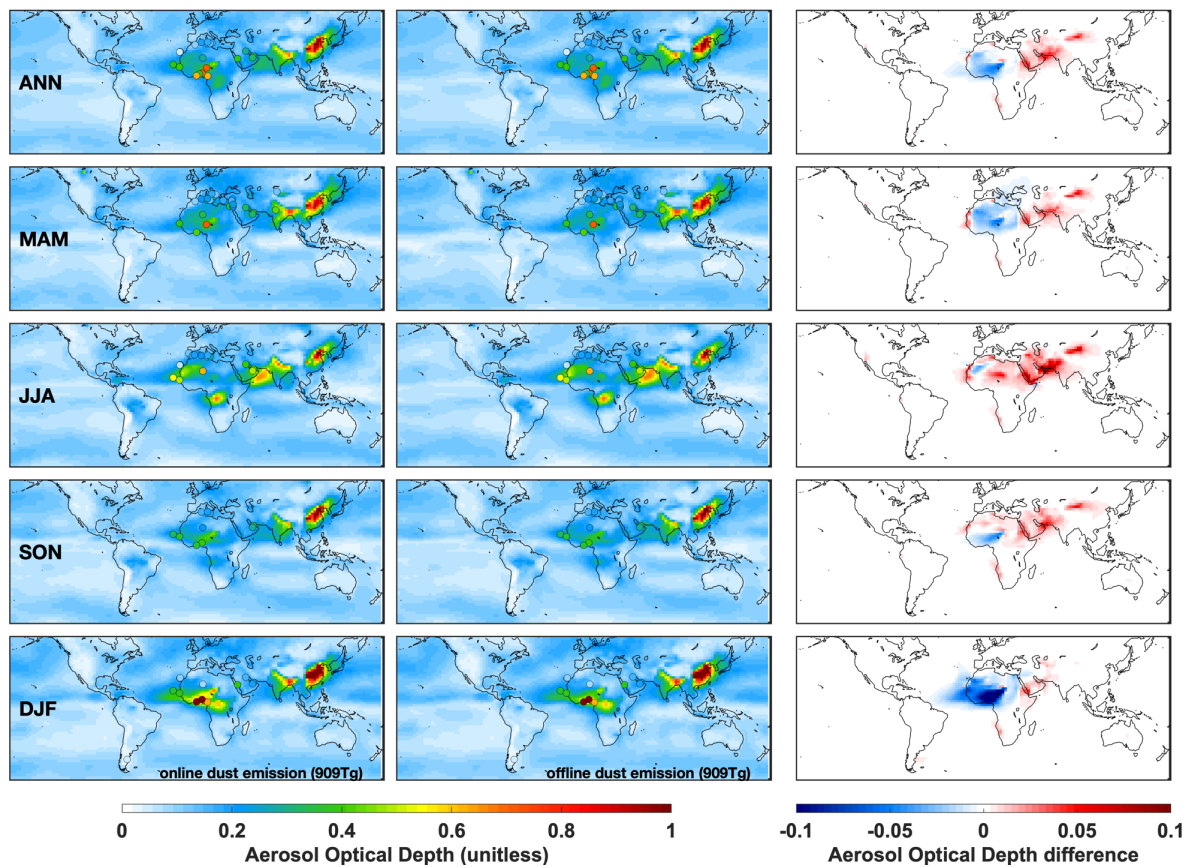


Figure S7. Spatial distribution of simulated AOD from simulations using the online dust emissions (left column) and offline dust emissions (middle column) that were with the same updated dust source function and the same annual dust strength (909 Tg), and the AOD differences between those two simulations (right column) in different seasons. Filled circles represent the AERONET measurements included in Figure 3.

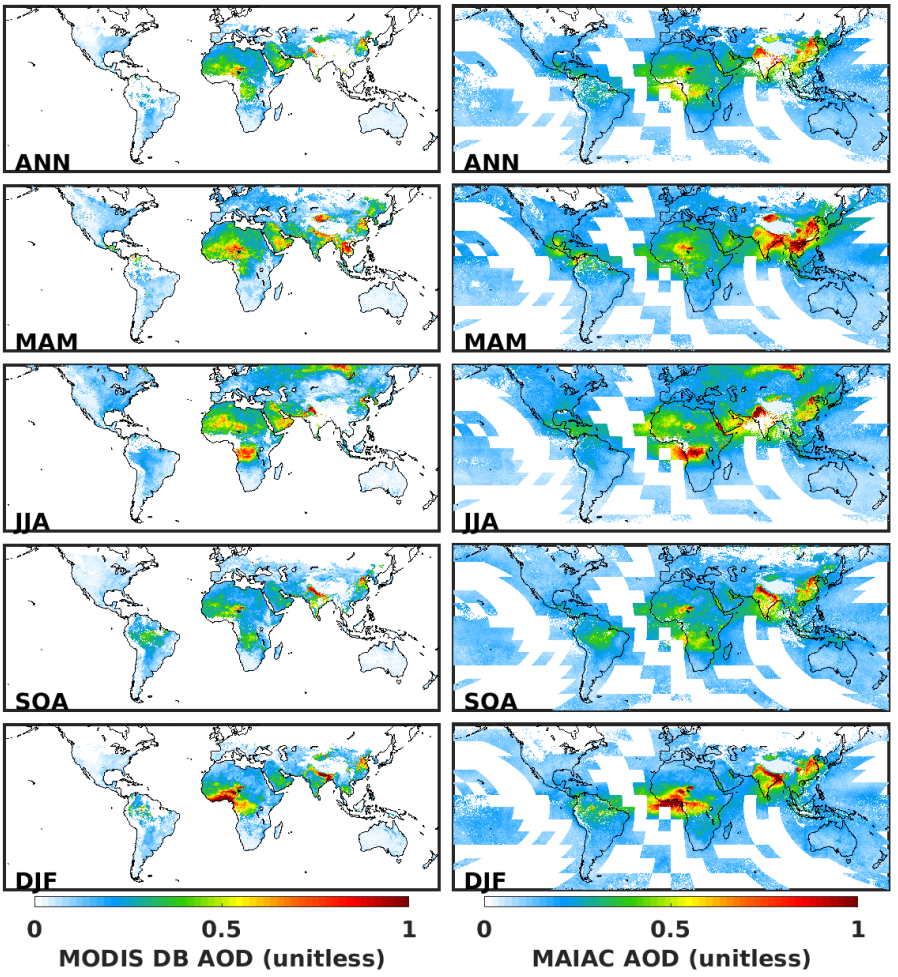


Figure S86. Annual and seasonal satellite AOD from MODIS Deep Blue (DB) and MAIAC algorithms.

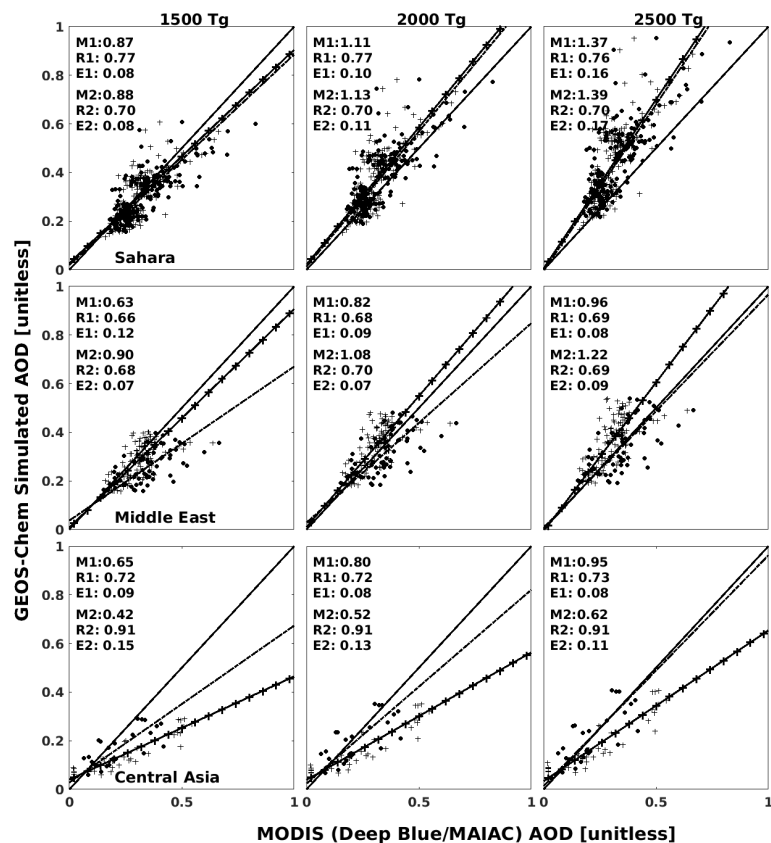


Figure S97. Scatter plots and statistics of comparing GEOS-Chem simulated annual mean AOD with satellite AOD over desert regions. Three columns represent three simulations with total annual dust emissions scaled to the value of 1,500 Tg, 2,000 Tg and 2,500 Tg respectively. The results for the Sahara, Middle East and central Asian deserts are shown in the top, middle and bottom rows respectively. Dots represent the comparison with MODIS Deep Blue AOD; the plus signs represent the comparison with MAIAC AOD. Correlation coefficient (R), root mean square error (E), and Slope (M) are reported, in which R1, E1 and M1 show the results of the comparison with MODIS Deep AOD; R2, E2 and M2 show the results of the comparison with MAIAC AOD. The best fit lines are lines with corresponding marker signs. The 1:1 line solid black line.

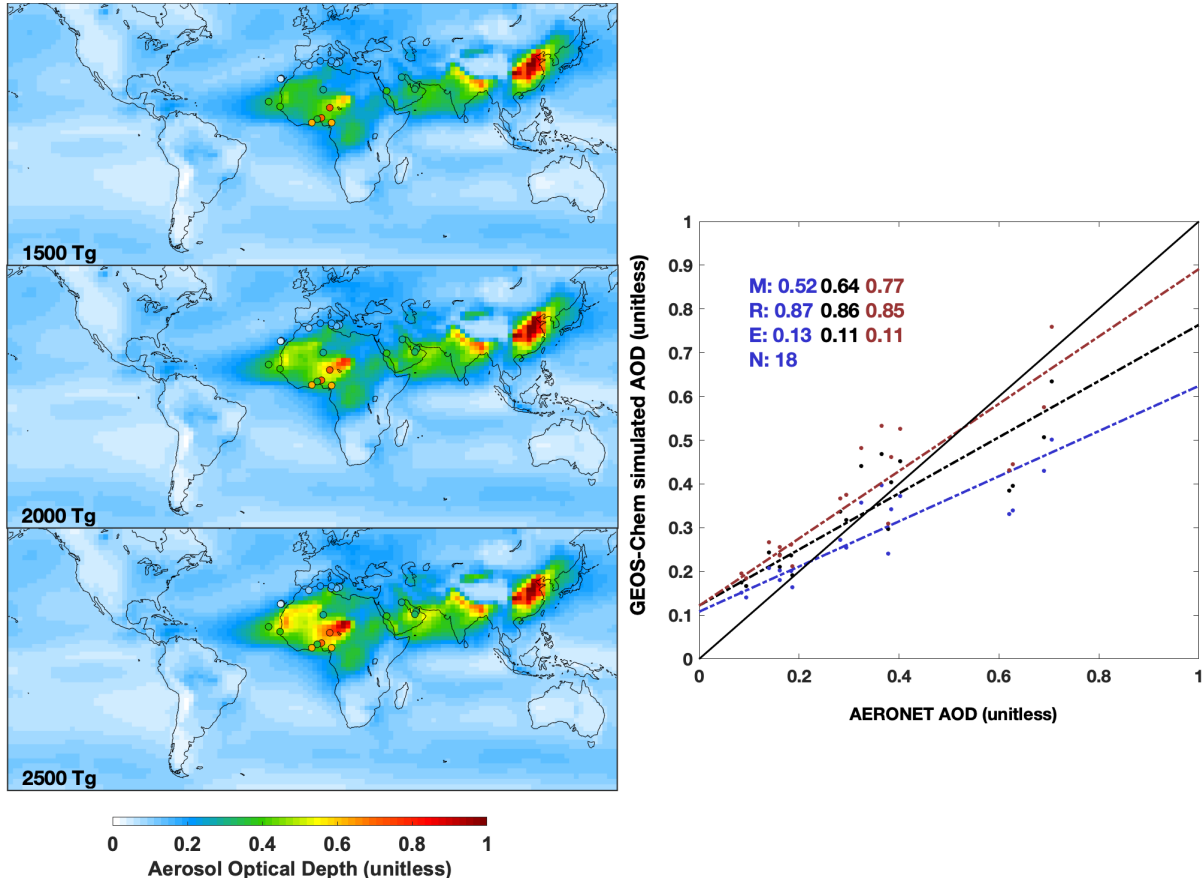


Figure S108. Annual mean simulated aerosol optical depth (AOD) from GEOS-Chem simulations for 2016 for simulations with total annual dust emissions of 1,500 Tg, 2,000 Tg and 2,500 Tg, and the comparison against AERONET measured AOD. Sites, shown as filled circles are chosen by where the ratio of simulated DOD and AOD exceeds 0.5. Corresponding statistics, including root mean square error (E), correlation coefficient (R) and slope (M), are inset. Blue, black and red in the scatter plot represent simulations with total annual dust emissions of 1,500 Tg, 2,000 Tg and 2,500 Tg, respectively.

## References

[Chinese Academy of Sciences, Chinese Desertification Map, Resource and Environment Database, Beijing, 1998.](#)

Defries, R. S., Hansen, M. C. and Townshend, J. R. G.: Global continuous fields of vegetation characteristics: A linear mixture model applied to multi-year 8 km AVHRR data, *International Journal of Remote Sensing*, 21(6–7), 1389–1414, <https://doi.org/10.1080/014311600210236>, 2000.

Ginoux, P., Chin, M., Tegen, I., Prospero, J. M., Holben, B., Dubovik, O. and Lin, S.-J.: Sources and distributions of dust aerosols simulated with the GOCART model, *Journal of Geophysical Research: Atmospheres*, 106(D17), 20255–20273, <https://doi.org/10.1029/2000JD000053>, 2001.

Gong, S. L., Zhang, X. Y., Zhao, T. L., McKendry, I. G., Jaffe, D. A. and Lu, N. M.: Characterization of soil dust aerosol in China and its transport and distribution during 2001 ACE-Asia: 2. Model simulation and validation, *Journal of Geophysical Research: Atmospheres*, 108(D9), <https://doi.org/10.1029/2002JD002633>, 2003.

White, B. R.: soil transport by winds on Mars, *Journal of Geophysical Research: Solid Earth*, 84(B9), 4643–4651, <https://doi.org/10.1029/JB084iB09p04643>, 1979.

Zender, C. S., Bian, H. and Newman, D.: Mineral Dust Entrainment and Deposition (DEAD) model: Description and 1990s dust climatology, *Journal of Geophysical Research: Atmospheres*, 108(D14), <https://doi.org/10.1029/2002JD002775>, 2003.